Spin-waves in itinerant ferromagnets

2001 J. Phys.: Condens. Matter 13 5327

(http://iopscience.iop.org/0953-8984/13/22/324)

INSTITUTE OF PHYSICS PUBLISHING JOURNAL OF PHYSICS: CONDENSED MATTER

J. Phys.: Condens. Matter **13** (2001) 5327–5352 www.iop.org/Journals/cm PII: S0953-8984(01)14087-7

Spin-waves in itinerant ferromagnets

J Bünemann

Fachbereich Physik, Universität Marburg, D-35032 Marburg, Germany

Received 22 May 2000, in final form 14 March 2001

Abstract

We introduce a novel approach for the investigation of spin-wave excitations in itinerant ferromagnets. Our theory is based on a variational treatment of general multi-band Hubbard models which describe elements and compounds of transition metals. The magnon dispersion is derived approximately as the energy of a variational spin-wave state in the limit of large spatial dimensions. A numerical evaluation of our results is feasible for general multi-band models. As a first application we consider a model with two degenerate orbitals per lattice site. From our results we can conclude that spin-wave excitations in strong itinerant ferromagnets are very similar to those in ferromagnetic spin systems.

1. Introduction

The most prominent examples of metals with a ferromagnetic order are the elements in the iron group, namely iron, cobalt and nickel. Although the magnetic behaviour of these materials is a well known phenomenon, there are still many open questions in this field (for a general introduction, see e.g., [1, 2]). It is generally accepted that the basic reason for ferromagnetic order is the interplay between the kinetic energy and the Coulomb interaction of the electrons. Nevertheless, it is still a matter of debate which kind of minimal model must be used for the description of ferromagnetic materials. Whatever an appropriate Hamilton may be, from a theoretical point of view one would expect that it will be a hard analytical task to find even an approximate solution for such a real many-particle problem.

The simplest theory which gives an explanation for metallic ferromagnetism is the Hartree–Fock–Stoner theory [3]. A surprising result of this theory is the statement that ferromagnetism occurs in any system provided that the product of Coulomb interactions and the electrons' density of states exceeds a certain amount. This statement is the famous Stoner criterion. This criterion usually leads to surprisingly small critical values of the Coulomb interaction for which ferromagnetism is predicted to occur. At first sight one may consider this as an *a posteriori* justification of the Hartree–Fock theory, which certainly fails for stronger Coulomb interactions. However, in some simpler model systems like the one-band Hubbard model it is well known that ferromagnetism requires very large Coulomb interactions if it exists at all. This is a definite contradiction to Hartree–Fock theory, which indicates that the whole Stoner picture may be inadequate for a thorough understanding of itinerant

0953-8984/01/225327+26$30.00

ferromagnetism. Similar objections could be raised against spin-density functional theory which, like Stoner theory, is based on an effective one-particle description. Despite their conceptual shortcomings, these theories quite successfully describe some properties of the iron group elements, i.e. the magnetic moment or the shapes of the multisheet Fermi surfaces [4]. Therefore, a competitive strong-coupling theory must meet these apparent successes of spin-density functional theory before it will be taken seriously.

To this end, we recently introduced a variational treatment of multi-band Hubbard models with a general class of Gutzwiller wave-functions [5, 6]. These models allow the description of real materials, for example the elements of the iron group. As a first application we studied the ferromagnetic transition in a two-band model. In contradiction to the Hartree–Fock theory we found that ferromagnetism requires quite large Coulomb interactions. In particular, we demonstrated the decisive role of the intra-atomic exchange interaction, which is found to be irrelevant in the Hartree–Fock approach. The Gutzwiller theory shows that finite values of this exchange interaction are essential for metallic ferromagnetism. Based on these results, we suggested that the complex atomic Coulomb interaction has to be taken seriously in theories on itinerant ferromagnetism. In particular, it appears to be essential to take into account exchange interactions which form local spins according to Hund's rule. We are presently calculating physical properties of the iron group elements from our correlated electron approach [7]. First results for nickel show that our method is able to resolve all major discrepancies between experiment and spin-density functional theory [8].

Experiments not only provide information about ground-state physics, but also yield insight into dynamical properties of materials. It is found that metallic and insulating ferromagnets behave similarly with respect to their low-energy spin excitations. In both cases, inelastic neutron-scattering experiments show pronounced gapless spin-wave excitations [9, 10]. The understanding of these excitations is very important since they govern the magnetic phase transition at finite temperatures [11]. Theoretical methods which allow the determination of spin-wave dispersions in Hubbard models are quite rare. It is obvious that a convincing description of spin excitations can only be obtained starting from a qualified theory for the ground state. However, almost all earlier theories on spin-wave excitations in ferromagnets are based on effective one-particle theories. Some of these theories lead to surprisingly accurate results compared to experiments. For example, in [12] a random-phase approximation for iron and nickel was introduced. In other approaches, the spin-wave dispersion is determined via a mapping of the itinerant system to a ferromagnetic Heisenberg model (see, e.g. [13]).

In this work, we present a theory for spin-wave excitations in itinerant ferromagnets which is based on the variational ground states in [6] (see also [14] as an earlier work where such an idea has been proposed). Our paper is organized as follows. In section 2 we introduce the general class of multi-band Hubbard models and the corresponding Gutzwiller wave functions. Our general approach on the spin-wave problem is presented in section 3. In section 4 we evaluate the spin-wave dispersion for our general class of multi-band Hubbard models. Finally, we apply our results to a model with two degenerate bands in section 5. A short conclusion closes our presentation. Technical details are given in four appendices.

2. Hamiltonian and variational wave function

2.1. Multi-band Hamiltonian

In this paper we consider the following general class of multi-band Hubbard models,

$$\hat{H} = \sum_{i(\neq)j} \sum_{\sigma,\sigma'} t_{i,j}^{\sigma,\sigma'} \hat{c}_{i;\sigma}^{+} \hat{c}_{j;\sigma'} + \sum_{i} \hat{H}_{i;\mathrm{at}} \equiv \hat{H}_1 + \hat{H}_{\mathrm{at}}. \tag{1}$$

Here, $\hat{c}^{+}_{i;\sigma}$ creates an electron with combined spin–orbit index $\sigma = 1, \ldots, 2N$ ($N = 5$ for 3d electrons) at the lattice site i of a solid. Inter-site correlations are generally neglected in Hubbard models. Their role for itinerant ferromagnetism is a controversial issue [15, 16]. We expect them to play a minor role for three-dimensional ferromagnetic systems.

For simplicity, we assume that the orbitals do not belong to the same representation of the respective point-symmetry group. For example, in cubic symmetry this means that there is only one set of s, p, e_g and t_{2g} orbitals. In this case, one-particle-states $|\Phi_0\rangle$, which respect the symmetry of the lattice, lead to vanishing non-diagonal local hopping-terms, i.e.

$$\left\langle \Phi_0 \middle| \hat{c}^{+}_{i,\sigma} \hat{c}_{i,\sigma'} \middle| \Phi_0 \right\rangle \sim \delta_{\sigma,\sigma'}. \tag{2}$$

This relation simplifies the calculations in this paper, but there is no fundamental obstacle to extend our method to a more general case.

We further assume that the atomic Hamiltonian

$$\hat{H}_{i;\mathrm{at}} = \sum_{\sigma} \epsilon_{\sigma} \hat{n}_{\sigma} + \sum_{\sigma_1,\sigma_2,\sigma_3,\sigma_4} \mathcal{U}^{\sigma_1,\sigma_2;\sigma_3,\sigma_4} \hat{c}^{+}_{\sigma_1} \hat{c}^{+}_{\sigma_2} \hat{c}_{\sigma_3} \hat{c}_{\sigma_4}. \tag{3}$$

is site-independent and readily diagonalized,

$$\hat{H}_{\mathrm{at}} = \sum_{\Gamma} E_{\Gamma} \hat{m}_{\Gamma} \tag{4a}$$

$$\hat{m}_{\Gamma} = |\Gamma\rangle \langle\Gamma| . \tag{4b}$$

Here, we introduced the eigenvalues E_Γ and the eigenstates $|\Gamma\rangle$ of $\hat{H}_{\mathrm{at}}$. The diagonalization of $\hat{H}_{\mathrm{at}}$ is a standard exercise (see e.g., [17]). Knowledge of the states $|\Gamma\rangle$ means that we found their expansion

$$|\Gamma\rangle = \sum_{I} T_{I,\Gamma} |I\rangle \tag{5}$$

in the basis of the configuration states $|I\rangle$. In these states, a definite set of spin–orbit states σ is occupied

$$|I\rangle = |\sigma_1, \sigma_2, \ldots\rangle = \hat{c}^{+}_{\sigma_1} \hat{c}^{+}_{\sigma_2} \cdots |\mathrm{vacuum}\rangle \qquad (\sigma_1 < \sigma_2 < \ldots). \tag{6}$$

For details about the notation, see [6], section 2.

2.2. Gutzwiller-wave-function and diagrammatic evaluation

In [6] we proposed the following wave-function for a variational examination of the Hamiltonian (1):

$$|\Psi_{\mathrm{G}}\rangle = \hat{P}_{\mathrm{G}} |\Phi_0\rangle = \prod_{i} \hat{P}_{i;\mathrm{G}} |\Phi_0\rangle. \tag{7}$$

Here, $|\Phi_0\rangle$ is any normalized single-particle product state and the local Gutzwiller projector $\hat{P}_{i;\mathrm{G}}$ is defined as

$$\hat{P}_{i;\mathrm{G}} = \prod_{\Gamma} \lambda_{\Gamma}^{\hat{m}_{\Gamma}} = 1 + \sum_{\Gamma} (\lambda_{\Gamma} - 1) \hat{m}_{\Gamma}. \tag{8}$$

To simplify our notation, we suppress the spatial indices wherever a misunderstanding is impossible, e.g., we omitted the index i on the right-hand-side of equation (8). The real variational parameters λ_Γ may have values between zero and one, where these two limits generate the ground-state both in the uncorrelated ($\hat{H}_{\mathrm{at}} = 0$) and the atomic limit ($\hat{H}_1 = 0$) of our Hamiltonian (1).

In [6] we showed that the expectation value of the Hamiltonian (1) can be evaluated for the wave-function (7) in the limit of infinite spatial dimensions. In this section we only summarize the main ideas of the diagrammatic derivation which are important for our treatment of the spin-wave-problem in the next sections. For all details we refer the reader to [6].

First, let us consider the norm of the wave-function (7),

$$\langle \Psi_{\mathrm{G}} \mid \Psi_{\mathrm{G}} \rangle = \prod_i \langle \Phi_0 | \hat{P}^2_{i;\mathrm{G}} | \Phi_0 \rangle. \tag{9}$$

The square of the local Gutzwiller-projector can be written as

$$\hat{P}^2_{i;\mathrm{G}} = 1 + \sum_{I,I'\,(|I|,|I'|\geqslant 2)} x_{i;I,I'} \hat{n}^{\mathrm{HF}}_{i;I,I'} \tag{10}$$

where we introduced the (local) Hartree–Fock-operators

$$\hat{n}^{\mathrm{HF}}_{I,I} = \prod_{\sigma\in I} \hat{n}^{\mathrm{HF}}_{\sigma} \tag{11a}$$

$$\hat{n}^{\mathrm{HF}}_{\sigma} = \hat{n}_{\sigma} - n^0_{\sigma} \tag{11b}$$

for $I = I'$, and

$$\hat{n}^{\mathrm{HF}}_{I,I'} = \hat{n}^{\mathrm{HF}}_{J,J} \hat{n}_{I_1,I_2} \qquad (J = I \cap I';\ I = J \cup I_1;\ I' = J \cup I_2) \tag{11c}$$

$$\hat{n}_{I_1,I_2} = \prod_{\sigma_1\in I_1} \hat{c}^{+}_{\sigma_1} \prod_{\sigma_2\in I_2} \hat{c}_{\sigma_2} \tag{11d}$$

for $I\ I$. The operators $\hat{c}^{+}_{\sigma_1}(\hat{c}_{\sigma_2})$ in (11d) should be placed in an ascending (descending) order. An explicit expression for the coefficients $x_{i;I,I'}$ in (10) is derived in appendix B.

When we apply Wick's theorem to the right-hand-side of equation (9), all terms are represented by certain diagrams with lines

$$P^{\sigma,\sigma'}_{i,j} = \langle \Phi_0 | \hat{c}^{+}_{i,\sigma} \hat{c}_{j,\sigma'} | \Phi_0 \rangle \tag{12}$$

and local vertices $x_{l;I,I'}$. The special form of the operator $\hat{P}^2_{i;\mathrm{G}}$ in (10) has two essential consequences for the structure of our diagrams. First, the definition of the Hartree–Fock operators together with equation (2) guarantees that there are no local lines, i.e.,

$$P^{\sigma,\sigma'}_{i,i} = 0. \tag{13}$$

Second, the constraint $|I|, |I'| \geqslant 2$ requires that at least four lines meet at every local vertex. When we evaluate the expectation values in

$$\langle \hat{H}_{i;\mathrm{at}} \rangle_{\Psi_{\mathrm{G}}} = \sum_{\Gamma} E_{\Gamma} \langle \hat{m}_{i;\Gamma} \rangle_{\Psi_{\mathrm{G}}} \tag{14a}$$

and

$$\langle \hat{H}_1 \rangle_{\Psi_{\mathrm{G}}} = \sum_{i,j;\sigma,\sigma'} t^{\sigma,\sigma'}_{i,j} \langle \hat{c}^{+}_{i;\sigma} \hat{c}_{j;\sigma'} \rangle_{\Psi_{\mathrm{G}}} \tag{14b}$$

we obtain diagrams, which contain one (for $\hat{H}_{i;\mathrm{at}}$) or two (for $\hat{H}_1$) external vertices for the lattice sites i (and j). If such a diagram possesses at least one internal vertex, we have lattice sites which are connected by more than two lines. Such diagrams vanish in infinite dimensions and therefore we concluded in [6] that the expectation values (14) only include diagrams without any internal vertex. Thus, we can write the expectation values $\langle \hat{m}_{\Gamma} \rangle_{\Psi_{\mathrm{G}}} = \langle \hat{m}_{i;\Gamma} \rangle_{\Psi_{\mathrm{G}}}$ in (14a) as

$$m_{\Gamma} \equiv \langle \hat{m}_{\Gamma} \rangle_{\Psi_{\mathrm{G}}} = \lambda^2_{\Gamma} m^0_{\Gamma} \equiv \lambda^2_{\Gamma} \langle \hat{m}_{\Gamma} \rangle_0 \tag{15}$$

with uncorrelated expectation values $\langle \ldots \rangle_0 \equiv \langle \ldots \rangle_{\Phi_0}$. This relation allows us to replace the original variational parameters λ_Γ by the new parameters m_Γ. The expectation value for a hopping term in (14*b*) becomes

$$\left\langle \hat{c}^+_{i;\sigma} \hat{c}_{j;\sigma'} \right\rangle_{\Psi_G} = \sqrt{q_\sigma q_{\sigma'}} \langle \hat{c}^+_{i;\sigma} \hat{c}_{j;\sigma'} \rangle_0 \tag{16a}$$

$$\sqrt{q_\sigma} \equiv \sqrt{\frac{1}{n^0_\sigma (1 - n^0_\sigma)}} \sum_{\Gamma,\Gamma'} \sqrt{\frac{m_\Gamma m_{\Gamma'}}{m^0_\Gamma m^0_{\Gamma'}}} \times \sum_{I,I'(\sigma \notin I,I')} f^I_\sigma \, f^{I'}_\sigma \sqrt{m^0_{(I' \cup \sigma)} m^0_{I'}} T^+_{\Gamma,(I\cup\sigma)} T_{(I'\cup\sigma),\Gamma} T^+_{\Gamma',I'} T_{I,\Gamma'}. \tag{16b}$$

Here, the fermionic sign function

$$f^I_\sigma \equiv \langle I \cup \sigma | \hat{c}^+_\sigma | I \rangle \tag{17}$$

gives a minus (plus) sign if it takes an odd (even) number of anticommutations to shift the operator $\hat{c}^+_\sigma$ to its proper place in the sequence of electron creation operators in $|I \cup \sigma\rangle$. Note that the numbers q_σ in (16*a*) are just the diagonal-elements of the matrix $q^{\sigma'}_\sigma$ introduced in [6], which is diagonal for our symmetry-restricted orbital basis (see Section 2.1).

3. Spin waves

The theoretical examination of spin-wave excitations requires the analysis of the imaginary part $\chi_T(\vec{q}, E)$ of the transversal susceptibility [18], which is given as the retarded two-particle Green function

$$G_T(\vec{q}, E) = \frac{1}{L} \langle\langle \hat{S}^+_{\vec{q}} ; \hat{S}^-_{\vec{q}} \rangle\rangle_E \tag{18a}$$

$$= -\frac{\mathrm{i}}{L} \int_0^\infty \mathrm{d}t \, \mathrm{e}^{\mathrm{i}Et} \langle \Psi_0 | [\hat{S}^+_{\vec{q}}(t), \hat{S}^-_{\vec{q}}(0)] | \Psi_0 \rangle. \tag{18b}$$

Here, we introduced the $\vec{q}$-dependent spin-flip operators

$$\hat{S}^+_{\vec{q}} = \sum_l \mathrm{e}^{\mathrm{i}\vec{q}\vec{R}_l} \hat{S}^+_l = \sum_{l,b} \mathrm{e}^{\mathrm{i}\vec{q}\vec{R}_l} \hat{c}^+_{l,b,\uparrow} \hat{c}_{l,b,\downarrow} \tag{19a}$$

$$\hat{S}^-_{\vec{q}} = (\hat{S}^+_{\vec{q}})^+ = \sum_{l,b} \mathrm{e}^{-\mathrm{i}\vec{q}\vec{R}_l} \hat{c}^+_{l,b,\downarrow} \hat{c}_{l,b,\uparrow} \tag{19b}$$

in the Heisenberg-picture, where the sum includes all (L) lattice sites l and orbitals b. The magnetic excitations of the system are represented by poles of the Green function $G_T(\vec{q}, E)$ with energies $E - E_0 > 0$. For our further analysis we expand the 'spin-wave state'

$$\left| \Psi^0_{\vec{q}} \right\rangle \equiv \hat{S}^-_{\vec{q}} \, |\Psi_0\rangle \tag{20}$$

in terms of exact energy-eigenstates

$$\left| \Psi^0_{\vec{q}} \right\rangle = \sum_n W_n \, |\Psi_n\rangle \tag{21}$$

$$\hat{H} \, |\Psi_n\rangle = E_n \, |\Psi_n\rangle \, . \tag{22}$$

The Lehmann-representation of (18*a*),

$$G_T(\vec{q}, E) = \frac{1}{L} \sum_n \left[\frac{\left| \left\langle \Psi_n \middle| \hat{S}^-_{\vec{q}} \middle| \Psi_0 \right\rangle \right|^2}{E - (E_n - E_0) + \mathrm{i}'\mathrm{s}} - \frac{\left| \left\langle \Psi_n \middle| \hat{S}^+_{\vec{q}} \middle| \Psi_0 \right\rangle \right|^2}{E + (E_n - E_0) + \mathrm{i}'\mathrm{s}} \right] \tag{23}$$

shows that there are poles in $G_T(\vec{q}, E)$ for the energies $E_n - E_0 > 0$ with weights $|W_n|^2$.

In a ferromagnetic system the state $|\ \Psi^0_{\vec{q}=\vec{0}}\rangle$ is also a ground state of $\hat{H}$, since the operator $\hat{S}^-_{\vec{q}=\vec{0}}$ just flips a spin in the spin-multiplet of the ground-state $|\Psi_0\rangle$. Therefore, we can conclude that $G_T(\vec{0}, E)$ has one isolated pole for $E - E_0 = 0$. Now we consider finite, but small values of $\vec{q}$, and assume that the expansion (21) is still dominated by a narrow distribution of low-energy states. This scenario explains the pronounced peak in $\chi_T(\vec{q}, E)$ for small values of E and $|\vec{q}|$, which is seen in experiments and interpreted as a spin-wave excitation (see, e.g., [10]). Then, the spin-wave dispersion $E_{\vec{q}}$ can be identified as the position of this peak, and $E_{\vec{q}}$ is approximately determined by the first moment of the distribution $|W_n|^2$,

$$E_{\vec{q}} = \frac{\sum_n E_n\,|W_n|^2}{\sum_n |W_n|^2} - \frac{\langle\Psi_0|\hat{H}|\Psi_0\rangle}{\langle\Psi_0\mid\Psi_0\rangle} \tag{24a}$$

$$= \frac{\langle\Psi_0|\hat{S}^+_{\vec{q}}\hat{H}\hat{S}^-_{\vec{q}}|\Psi_0\rangle}{\langle\Psi_0|\hat{S}^+_{\vec{q}}\hat{S}^-_{\vec{q}}|\Psi_0\rangle} - \frac{\langle\Psi_0|\hat{H}|\Psi_0\rangle}{\langle\Psi_0\mid\Psi_0\rangle}. \tag{24b}$$

Here, we assumed that the contribution of high-energy ('Stoner')-excitations is negligible.

It is still impossible to derive the spin-wave dispersion $E_{\vec{q}}$ from equation (24) since we do not know the ground-state $|\Psi_0\rangle$ of our multi-band Hamiltonian (1). If we assume, however, that the variational wave function $|\Psi_{\rm G}\rangle$ is a good approximation for the true ground-state $|\Psi_0\rangle$ we may substitute $|\Psi_0\rangle$ in equation (24) by the variational wave function $|\Psi_{\rm G}\rangle$.

In the next section we will evaluate the 'variational' spin-wave dispersion

$$E^{var}_{\vec{q}} = \frac{\langle\Psi_{\rm G}|\hat{S}^+_{\vec{q}}\hat{H}\hat{S}^-_{\vec{q}}|\Psi_{\rm G}\rangle}{\langle\Psi_{\rm G}|\hat{S}^+_{\vec{q}}\hat{S}^-_{\vec{q}}|\Psi_{\rm G}\rangle} - \frac{\langle\Psi_{\rm G}|\hat{H}|\Psi_{\rm G}\rangle}{\langle\Psi_{\rm G}\mid\Psi_{\rm G}\rangle} \tag{25}$$

in the limit of large spatial dimensions. It should be noted that this quantity obviously obeys no strict upper-bound properties. Nevertheless, we expect that $E^{\rm exp}_{\vec{q}} < E^{var}_{\vec{q}}$ is fulfilled since the expectation values (24) include high-energy states which do not belong to the spin-wave excitation seen in experiments.

In principle, transversal spin-excitations are given as peaks both in $\chi_T(\vec{q}, E)$ and $\chi_T(\vec{q}, E_0 - E)$ for energies $E > E_0$. In other words, we also had to consider the contributions from the Green function $\langle\langle\hat{S}^-_{\vec{q}}\,;\,\hat{S}^+_{\vec{q}}\rangle\rangle_E$ in our calculation. These contributions are identical to the second term in equation (23) and we could include them by using the proper spin-wave state

$$|\tilde{\Psi}^0_{\vec{q}}\rangle \equiv \left(\hat{S}^-_{\vec{q}} + \hat{S}^+_{\vec{q}}\right)|\Psi_G\rangle \tag{26}$$

in our variational approach. However, the contributions from the second operator in (26) vanish for $\vec{q} = \vec{0}$ and may be neglected for small values of $|\vec{q}|$, where spin-wave excitations are observed in experiments. Nevertheless, there is no fundamental obstacle to extending our diagrammatic approach to the more general spin-wave state (26).

4. Variational spin-wave dispersion

4.1. General considerations

In order to determine the variational spin-wave dispersion (25) we need to examine the norm of the state $|\Psi^{\rm G}_{\vec{q}}\rangle \equiv \hat{S}^-_{\vec{q}}|\Psi_{\rm G}\rangle$,

$$N_{\vec{q}} \equiv \langle\Psi_{\rm G}|\ \hat{S}^+_{\vec{q}}\hat{S}^-_{\vec{q}}\ |\Psi_{\rm G}\rangle \tag{27}$$

and the expectation values

$$\frac{\langle\Psi_{\vec{q}}^{\mathrm{G}}|\hat{H}_{\mathrm{at}}|\Psi_{\vec{q}}^{\mathrm{G}}\rangle}{N_{\vec{q}}} = \sum_{\Gamma} E_{\Gamma} \sum_{i,j,k} \mathrm{e}^{\mathrm{i}\vec{q}(\vec{R}_i-\vec{R}_j)} \frac{\langle\Psi_{\mathrm{G}}|\hat{S}_i^{+}\hat{m}_{k;\Gamma}\hat{S}_j^{-}|\Psi_{\mathrm{G}}\rangle}{N_{\vec{q}}} \tag{28a}$$

$$\frac{\langle\Psi_{\vec{q}}^{\mathrm{G}}|\hat{H}_{1}|\Psi_{\vec{q}}^{\mathrm{G}}\rangle}{N_{\vec{q}}} = \sum_{i,j,k,l} \mathrm{e}^{\mathrm{i}\vec{q}(\vec{R}_i-\vec{R}_j)} \sum_{\sigma_k,\sigma_l} t_{k,l}^{\sigma_k,\sigma_l} \frac{\langle\Psi_{\mathrm{G}}|\hat{S}_i^{+}\hat{c}_{k;\sigma_k}^{+}\hat{c}_{l;\sigma_l}\hat{S}_j^{-}|\Psi_{\mathrm{G}}\rangle}{N_{\vec{q}}}. \tag{28b}$$

Before we start to evaluate these quantities, it is necessary to discuss two general problems. First, let us consider the norm

$$N_{\vec{q}} = \sum_{i,j,b,b'} \mathrm{e}^{\mathrm{i}\vec{q}(\vec{R}_i-\vec{R}_j)} \langle\Psi_{\mathrm{G}}|\hat{c}_{i,b,\uparrow}^{+}\hat{c}_{i,b,\downarrow}\hat{c}_{j,b',\downarrow}^{+}\hat{c}_{j,b',\uparrow}|\Psi_{\mathrm{G}}\rangle \tag{29}$$

in the special case $\vec{q}=\vec{0}$, where $\hat{S}_{\vec{q}=\vec{0}}^{-}$ is just the total spin-flip operator $\hat{S}^{-}$. When we assume that $|\Psi_{\mathrm{G}}\rangle$ has the correct spin-symmetry, i.e. it is an eigenstate of

$$\hat{S}^{z} = \sum_{i} \hat{S}_{i,z} \qquad \text{and} \qquad \hat{\vec{S}}^{2} = \left(\sum_{i} \vec{S}_i\right)^{2} \tag{30}$$

with eigenvalues S_{G}^{z} and $S_{\mathrm{G}}^{z}(S_{\mathrm{G}}^{z}+1)$, respectively, we obtain

$$N_{\vec{q}=\vec{0}} = 2S_{\mathrm{G}}^{z}\ \langle\Psi_{\mathrm{G}}\mid\Psi_{\mathrm{G}}\rangle\,. \tag{31}$$

Here, we used the well known equation

$$\hat{S}^{+}\hat{S}^{-} = \hat{\vec{S}}^{2} - \hat{S}^{z}(\hat{S}^{z}-1) \tag{32}$$

for spin operators. In general, however, the wave functions $|\Psi_{\mathrm{G}}\rangle$, as defined in equation (8), do not fulfill this symmetry. Therefore, it is necessary to introduce some additional constraints on our variational parameters λ_{Γ} in (8) to guarantee that $|\Psi_{\mathrm{G}}\rangle$ is an eigenstate of $\hat{\vec{S}}^{2}$. In appendix A we explain how these relations may be chosen.

The second problem arises from the evaluation of $\vec{q}$-dependent quantities in the limit of large spatial dimensions D. For example, let us consider the Hartree–Fock case, where $|\Psi_{\mathrm{G}}\rangle = |\Phi_0\rangle$ is a spin-polarized one-particle state with $n_{\uparrow} > n_{\downarrow}$. We find

$$\frac{N_{\vec{q}}^{0}}{L} = \frac{1}{L}\sum_{b,b'}\sum_{i,j} \mathrm{e}^{\mathrm{i}\vec{q}(\vec{R}_i-\vec{R}_j)} \langle\Phi_0|\hat{c}_{i,b,\uparrow}^{+}\hat{c}_{i,b,\downarrow}\hat{c}_{j,b',\downarrow}^{+}\hat{c}_{j,b',\uparrow}|\Phi_0\rangle \tag{33a}$$

$$= \sum_{b}\left(n_{b,\uparrow}^{0}(1-n_{b,\downarrow}^{0}) - \frac{1}{L}\sum_{i\neq j} \mathrm{e}^{\mathrm{i}\vec{q}(\vec{R}_i-\vec{R}_j)} P_{i,j}^{(b,\uparrow),(b,\uparrow)} P_{j,i}^{(b,\downarrow),(b,\downarrow)}\right) \tag{33b}$$

where, for simplicity, we assumed that the expectation-values $P_{i,j}^{\sigma,\sigma'}$ as defined in (12) are diagonal with respect to the orbitals b, b'. For any finite and generic value of $\vec{q}$ the sum in equation (33b) vanishes as $1/D$. This can be shown in momentum space when we further use that [19, 20]

$$\frac{1}{L}\sum_{k} n_{\vec{k}+\vec{q}}^{b} n_{\vec{k}}^{b'} = n_b n_{b'} + O(1/D).$$

Therefore the limits $\vec{q}\to 0$ and $D\to\infty$ do not commute, since

$$\lim_{\vec{q}\to\vec{0}}\lim_{D\to\infty}\frac{N_{\vec{q}}^{0}}{L} = \sum_{b} n_{b,\uparrow}^{0}\left(1-n_{b,\downarrow}^{0}\right) \neq \sum_{b}\left(n_{b,\uparrow}^{0}-n_{b,\downarrow}^{0}\right) = \lim_{D\to\infty}\lim_{\vec{q}\to\vec{0}}\frac{N_{\vec{q}}^{0}}{L}. \tag{34}$$

To overcome this problem we will evaluate expressions like the sum in (33*b*) using the realistic three-dimensional band-structure of our Hamiltonian (1). This leads to results which are continuous in $\vec{q}$ and, consequently, reproduce the limit $\vec{q} = \vec{0}$ correctly.

The norm of the state (7) for a correlated wave function $|\Psi_G\rangle \neq |\Phi_0\rangle$ will contain diagrams of an arbitrary order $1/D^n$. In this paper we will only consider diagrams up to the leading order $n = 1$. At first sight one may wonder whether or not $1/D$-terms need to be included in the ground-state energy expression as well. Fortunately, to order $1/D$, these diagrams only lead to a constant shift of the energy expectation-values for $|\Psi_G\rangle$ and $|\Psi^G_{\vec{q}}\rangle$. Thus, for our calculation we may neglect the $1/D$-contributions to the ground-state energy since we are only interested in the difference between these two energies.

In the next subsection we evaluate the norm (29). The derivation of the expectation values (28*a*) and (28*b*) requires no additional techniques. The cumbersome calculations are given in appendices C and D.

4.2. Evaluation of the norm

The norm of the state (27) can be written as

$$N_{\vec{q}} = \sum_i \left\langle \left(\hat{P}_{i;G}\hat{S}^+_i\hat{S}^-_i\hat{P}_{i;G}\right) \prod_{l(\neq i)} \hat{P}^2_{l;G} \right\rangle_{\Phi_0} + \sum_{i\neq j} e^{i\vec{q}(\vec{R}_i-\vec{R}_j)} \left\langle \left(\hat{P}_{i;G}\hat{S}^+_i\hat{P}_{i;G}\right)\left(\hat{P}_{j;G}\hat{S}^-_j\hat{P}_{j;G}\right) \prod_{l(\neq i,j)} \hat{P}^2_{l;G} \right\rangle_{\Phi_0} . \tag{35}$$

When we use equation (10) and apply Wick's theorem, we obtain diagrams with external vertices for the lattice sites i and j and internal vertices generated by the Hartree–Fock operators $x_{l;I,I'}\hat{n}^{HF}_{l;I,I'}$ in $\hat{P}^2_{l;G}$. In [6, 21] it was shown that we only have to evaluate the connected diagrams since the unconnected terms just give the norm of the Gutzwiller wavefunction $N_G \equiv \langle\Psi_G \mid \Psi_G\rangle$. For the evaluation of the first line (35) we use the local relations

$$\hat{S}^+\hat{S}^- = \sum_\Gamma S_-(\Gamma)\hat{m}_\Gamma \tag{36a}$$

$$S_\pm(\Gamma) \equiv S(\Gamma)\left[S(\Gamma)+1\right] - S_z(\Gamma)\left[S_z(\Gamma)\pm 1\right] \tag{36b}$$

which follow from equation (32). Here, we introduced the total spin $S(\Gamma)$ and the spin-component $S_z(\Gamma)$ of the atomic eigenstates $|\Gamma\rangle$. Hence, the expectation value of $\hat{S}^+_i\hat{S}^-_i$ is given as a linear function of the variational parameters m_Γ and we may write (35) as

$$\frac{N_{\vec{q}}}{LN_G} = \sum_\Gamma S_-(\Gamma)m_\Gamma \tag{37a}$$

$$+ \sum_{i\neq j} e^{i\vec{q}(\vec{R}_i-\vec{R}_j)} \left\{ \left(\hat{P}_{i;G}\hat{S}^+_i\hat{P}_{i;G}\right)\left(\hat{P}_{j;G}\hat{S}^-_j\hat{P}_{j;G}\right) \prod_{l(\neq i,j)} \hat{P}^2_{l;G} \right\}^c_{\Phi_0} \tag{37b}$$

where $\{\ldots\}^c_{\Phi_0}$ denotes the application of Wick's theorem and taking into account only the connected diagrams.

For a further analysis of (37*b*) we introduce indices $\mathfrak{D} = (\sigma_1\sigma_2)$ for pairs of spin–orbit states σ_i and the basic RPA-diagrams

$$\tilde{P}^{\mathfrak{D}'}_{\mathfrak{D}}(\vec{q}) = \tilde{P}^{(\sigma_1\sigma_2)}_{(\sigma_3\sigma_4)}(\vec{q}\,) \equiv -\frac{1}{L}\sum_{i\neq j} e^{i\vec{q}(\vec{R}_i-\vec{R}_j)} P^{\sigma_1\sigma_4}_{i,j} P^{\sigma_3\sigma_2}_{j,i}. \tag{38}$$

$\tilde{P}^{\mathfrak{D}'}_{\mathfrak{D}}(\vec{q})$ can be evaluated in momentum space as

$$\tilde{P}^{\mathfrak{D}'}_{\mathfrak{D}}(\vec{q}) = \delta^{\sigma_4}_{\sigma_1}\delta^{\sigma_2}_{\sigma_3} n^0_{\sigma_1} n^0_{\sigma_2} - \frac{1}{L}\sum_{\vec{k}} n^{\sigma_1\sigma_4}_{\vec{k}} n^{\sigma_3\sigma_2}_{\vec{k}+\vec{q}} \tag{39}$$

with expectation values

$$n^{\sigma\sigma'}_{\vec{k}} \equiv \left\langle \hat{c}^{+}_{\vec{k}\sigma}\hat{c}_{\vec{k}\sigma'}\right\rangle_{\Phi_0} \tag{40}$$

and a modified Kronecker-symbol $\delta^{\sigma'}_{\sigma} = \delta_{\sigma,\sigma'}$. Note that, in contrast to the indices I, the order of the two spin–orbit states in $\mathfrak{D} = (\sigma_1\sigma_2)$ is significant. Here, its first and second element specify a particle which enters or leaves a vertex, respectively.

For large spatial dimensions (i.e., up to the order $1/D$), the only contributions in (37b) are RPA-type diagrams as shown in figure 1. The internal vertices $\tilde{x}^{\mathfrak{D}'}_{\mathfrak{D}}$ are generated by the operators $\hat{P}^2_{l;\mathrm{G}}$, which can be expressed in terms of Hartree–Fock operators $x_{l;I,I'}\hat{n}^{\mathrm{HF}}_{l;I,I'}$ (see equation (10)). For our RPA-diagrams we only have to consider two-fermion-operators in $\hat{n}^{\mathrm{HF}}_{l;I,I'}$. A general vertex with n incoming and outgoing lines is determined by the operator

$$\begin{aligned}\sum_{I_1,I_2(I_1\cap I_2=\emptyset)}\ \sum_{J(I_1,I_2\notin J)} & x_{J\cup I_1,J\cup I_2}\left\{\ldots\hat{n}^{\mathrm{HF}}_{J\cup I_1,J\cup I_2}\ldots\right\}^c_{\Phi_0} \\ \rightarrow & \sum_{I_1,I_2(I_1\cap I_2=\emptyset)}\ \sum_{J(I_1,I_2\notin J)} y_{J\cup I_1,J\cup I_2}\left\{\ldots\hat{n}_{J\cup I_1,J\cup I_2}\ldots\right\}^c_{\Phi_0}\end{aligned} \tag{41}$$

with

$$y_{J\cup I_1,J\cup I_2} = x_{J\cup I_1,J\cup I_2} f^J_{I_1} f^J_{I_2}. \tag{42}$$

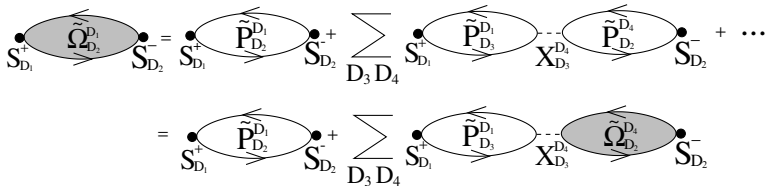

Figure 1. Multi-orbital RPA-diagrams for the matrix $\tilde{\Omega}$.

Thus, the internal vertex $\tilde{x}^{\mathfrak{D}'}_{\mathfrak{D}} = \tilde{x}^{(\sigma_1\sigma_2)}_{(\sigma_3\sigma_4)}$ with $\sigma_1 \neq \sigma_3$ and $\sigma_2 \neq \sigma_4$ at lattice site l stems from the term

$$y_{l;(\sigma_1,\sigma_3)(\sigma_2,\sigma_4)}\left\{\ldots\left(\hat{c}^{+}_{l,\sigma_1}\hat{c}_{l,\sigma_2}\right)\left(\hat{c}^{+}_{l,\sigma_3}\hat{c}_{l,\sigma_4}\right)\ldots\right\}^c_{\Phi_0} f^{\sigma_3}_{\sigma_1} f^{\sigma_4}_{\sigma_2}. \tag{43}$$

The round brackets indicate that Wick's theorem may not be applied to operators in different brackets. Thus, we can identify $\tilde{x}^{\mathfrak{D}'}_{\mathfrak{D}}$ as

$$\tilde{x}^{\mathfrak{D}'}_{\mathfrak{D}} = \tilde{x}^{(\sigma_1\sigma_2)}_{(\sigma_3\sigma_4)} = f^{\sigma_4}_{\sigma_2} f^{\sigma_3}_{\sigma_1} y_{(\sigma_1,\sigma_3),(\sigma_2,\sigma_4)}. \tag{44}$$

An explicit expression for $x_{I,I'}$ is derived in appendix B. Note that $\tilde{x}^{(\sigma_1\sigma_2)}_{(\sigma_3\sigma_4)} = 0$ if $\sigma_1 = \sigma_3$ or $\sigma_2 = \sigma_4$ per definition.

Our infinite RPA-sum (see figure 1) for the second term in (37b) leads to the following matrix-equation for $\tilde{\Omega}^{\mathfrak{D}'}_{\mathfrak{D}}(\vec{q}\,)$,

$$\tilde{\Omega}(\vec{q}\,) \equiv \tilde{P}(\vec{q}\,) + \tilde{P}(\vec{q}\,)\cdot\tilde{x}\cdot\tilde{P}(\vec{q}\,) + \tilde{P}(\vec{q}\,)\cdot\tilde{x}\cdot\tilde{P}(\vec{q}\,)\cdot\tilde{x}\cdot\tilde{P}(\vec{q}\,) + \ldots \tag{45a}$$

$$= \tilde{P}(\vec{q}\,) + \tilde{P}(\vec{q}\,)\cdot\tilde{x}\cdot\tilde{\Omega}(\vec{q}\,), \tag{45b}$$

which has the solution

$$\tilde{\Omega}(\vec{q}\,) = (\hat{1} - \tilde{P}(\vec{q}\,)\cdot\tilde{x})^{-1}\cdot\tilde{P}(\vec{q}\,). \tag{46}$$

Here, the dot '$\cdot$' indicates the usual product between two matrices.

Finally, we have to examine the external vertices, generated by the spin-operators $\hat{S}_i^+$ and $\hat{S}_j^-$ in (37*b*). First, we find for local operators

$$\hat{P}_{\mathrm{G}} S^+ \hat{P}_{\mathrm{G}} = \sum_{\Gamma',\Gamma} \lambda_{\Gamma'}\lambda_{\Gamma} \left|\Gamma'\right\rangle\left\langle\Gamma'\right| S^+ \left|\Gamma\right\rangle \left\langle\Gamma\right| \tag{47a}$$

$$= \sum_{\Gamma} \lambda_{\Gamma_+}\lambda_{\Gamma}\sqrt{S_+(\Gamma)}\left|\Gamma_+\right\rangle \left\langle\Gamma\right| \tag{47b}$$

where the normalized spin-flip-states

$$\left|\Gamma_\pm\right\rangle \equiv \frac{1}{\sqrt{S_\pm(\Gamma)}}\hat{S}^\pm \left|\Gamma\right\rangle \tag{48}$$

were introduced. We may write equation (47*b*) as

$$\hat{P}_{\mathrm{G}} S^+ \hat{P}_{\mathrm{G}} = \sum_{\Gamma} \lambda_{\Gamma_+}\lambda_{\Gamma}\sqrt{S_+(\Gamma)} \sum_{I_1,I_2} T_{I_1,\Gamma_+} T^+_{\Gamma,I_2} \hat{m}_{I_1,I_2} \tag{49}$$

with

$$\hat{m}_{I_1,I_2} = f_I^J\, f_{I'}^J \hat{m}_J^{I,I'}\, \hat{n}_{I,I'} \tag{50a}$$

$$\hat{m}_J^{I,I'} \equiv \prod_{\sigma\in J} \hat{n}_\sigma \prod_{\sigma\in\bar{J}\setminus(I\cup I')} (1-\hat{n}_\sigma) \tag{50b}$$

and $J = I_1 \cap I_2$, $I_1 = J \cup I$, $I_2 = J \cup I'$.

The external vertices in our RPA-diagrams are met by just two lines. Therefore, we only need the following one-particle contribution of the operator $\hat{m}_{I_1,I_2}$ in (49),

$$\left\{\ldots \hat{m}_{I_1,I_2} \ldots\right\}^C_{\Phi_0} \to \sum_{\sigma_1,\sigma_2} \mathfrak{V}^{(\sigma_1\sigma_2)}_{I_1,I_2} \left\{\ldots \hat{c}^+_{\sigma_1}\hat{c}_{\sigma_2}\ldots\right\}^c_{\Phi_0} \tag{51}$$

$$\mathfrak{V}^{(\sigma_1\sigma_2)}_{I_1,I_2} \equiv \sum_{J(\sigma_1,\sigma_2\notin J)} f^J_{\sigma_1}\, f^J_{\sigma_2} m^0_J \Big(\prod_{\sigma\in(\sigma_1,\sigma_2)} \frac{1}{(1-n^0_\sigma)}\Big)\Big[\delta^{J\cup\sigma_1}_{I_1}\delta^{J\cup\sigma_2}_{I_2,} - \delta^{\sigma_2}_{\sigma_1}\delta^J_{I_1}\delta^J_{I_2}\Big]$$

where we assumed that $|I_1| = |I_2|$. When we apply this result to the contribution of the external vertex (37*b*), we only need to consider the first term with $\sigma_1 \neq \sigma_2$, because σ_1, σ_2 must have different spins. Thus, the expression for the external vertex, which stems from $\hat{S}_i^+$ becomes

$$S^+_{(\sigma_1\sigma_2)} = \sum_{\Gamma} \lambda_{\Gamma_+}\lambda_{\Gamma}\sqrt{S_+(\Gamma)} \sum_{I_1,I_2} T_{I_1,\Gamma_+} T^+_{\Gamma,I_2} \mathfrak{V}^{(\sigma_1\sigma_2)}_{I_1,I_2} \tag{52a}$$

$$= \sum_{\Gamma} \lambda_{\Gamma_+}\lambda_{\Gamma}\sqrt{S_+(\Gamma)} \sum_{J(\sigma_1,\sigma_2\notin J)} T_{J\cup\sigma_1,\Gamma_+} T^+_{\Gamma,J\cup\sigma_2} \frac{f^J_{\sigma_1}\, f^J_{\sigma_2} m^0_J}{(1-n^0_{\sigma_1})(1-n^0_{\sigma_2})}. \tag{52b}$$

The expansion

$$\left\{\ldots \hat{P}_{\mathrm{G}}\hat{S}^-\hat{P}_{\mathrm{G}}\ldots\right\}^C_{\Phi_0} \to \sum_{\sigma_1,\sigma_2} \left[S^+_{(\sigma_1\sigma_2)} \left\{\ldots\left(\hat{c}^+_{\sigma_1}\hat{c}_{\sigma_2}\right)\ldots\right\}^c_{\Phi_0}\right]^* \tag{53a}$$

$$= \sum_{\sigma_1,\sigma_2} \left(S^+_{(\sigma_1\sigma_2)}\right)^* \left\{\ldots\left(\hat{c}^+_{\sigma_2}\hat{c}_{\sigma_1}\right)\ldots\right\}^c_{\Phi_0} \tag{53b}$$

shows that the vertex-factor for the operator $\hat{S}_j^-$ in (37*b*) is given as

$$S^-_{(\sigma_1\sigma_2)} = \left(S^+_{(\sigma_2\sigma_1)}\right)^* . \tag{54}$$

When we consider $S^+_{\mathfrak{D}}$ and $S^-_{\mathfrak{D}}$ as components of vectors $\vec{S}^+$ and $\vec{S}^-$ with respect to the indices $\mathfrak{D}$ we obtain the following final result for the norm $N_{\vec{q}}$

$$\frac{N_{\vec{q}}}{LN_{\mathrm{G}}} = \sum_{\Gamma} S_-(\Gamma) m_\Gamma + \sum_{\mathfrak{D}_1,\mathfrak{D}_2} S^+_{\mathfrak{D}_1}\, \tilde{\Omega}^{\mathfrak{D}_1}_{\mathfrak{D}_2}(\vec{q}\,)\, S^-_{\mathfrak{D}_2} \tag{55a}$$

$$= \sum_{\Gamma} S_-(\Gamma) m_\Gamma + \vec{S}^+ \cdot \tilde{\Omega}(\vec{q}\,) \cdot \vec{S}^- . \tag{55b}$$

Note that the norm N_G in (55*a*) will cancel out when we calculate the expectation values (28).

A similar derivation gives us the expectation values (28) of the kinetic energy and the Coulomb interaction, see appendices C and D. There, the number of contributing diagrams is much larger (e.g., 18 for the kinetic energy) since we have up to four external vertices. Nevertheless, the numerical evaluation of these terms is a minor technical problem as soon as the wave-function $|\Psi_{\mathrm{G}}\rangle$ has been determined by the minimization of our variational energy expression. First studies show that the application of our variational scheme to iron and nickel represents a solvable numerical task [7]. Further work in this direction is in progress.

5. Application to a two-band model

In this section we will present the results for the spin-wave properties in a system with two degenerate e_g-type orbitals per lattice site. The appearance of ferromagnetism in this model has already been discussed in [6], both for the Hartree–Fock and the Gutzwiller theory. Thus, we will only summarize these results here, before we start to consider the spin-wave dispersion. For all details, we refer to [6].

5.1. Ferromagnetic properties

In a system with two degenerate e_g orbitals the general atomic Hamiltonian (3) becomes

$$\hat{H}_{\mathrm{at}} = U \sum_b \hat{n}_{b,\uparrow}\hat{n}_{b,\downarrow} + U' \sum_{\sigma,\sigma'} \hat{n}_{1,\sigma}\hat{n}_{2,\sigma'} - J \sum_{\sigma} \hat{n}_{1,\sigma}\hat{n}_{2,\sigma} \tag{56}$$

$$+ J \sum_{\sigma} \hat{c}^+_{1,\sigma}\hat{c}^+_{2,-\sigma}\hat{c}_{1,-\sigma}\hat{c}_{2,\sigma} + J_{\mathrm{C}}\left(\hat{c}^+_{1,\uparrow}\hat{c}^+_{1,\downarrow}\hat{c}_{2,\downarrow}\hat{c}_{2,\uparrow} + \hat{c}^+_{2,\uparrow}\hat{c}^+_{2,\downarrow}\hat{c}_{1,\downarrow}\hat{c}_{1,\uparrow}\right).$$

In cubic symmetry the Coulomb- and exchange-integrals U, U', J and J_{C} are not independent from each other. Instead we have only two free parameters, because the relations $J = J_{\mathrm{C}}$ and $U - U' = 2J$ hold. For the determination of the optimal variational wave-function (7), we need the 16 eigenstates of the atomic Hamiltonian. The latter can be found in table 1 of [6].

In the one-particle Hamiltonian $\hat{H}_1$ we take into account first- and second-nearest-neighbour hopping matrix elements. Furthermore, we apply the two-centre approximation for the hopping matrix elements, which are chosen as $t^{(1)}_{dd\sigma} = 1$ eV, $t^{(2)}_{dd\sigma} = 0.25$ eV, and $t^{(1),(2)}_{dd\sigma} : t^{(1),(2)}_{dd\pi} : t^{(1),(2)}_{dd\delta} = 1 : (-0.3) : 0.1$ (see [22] for the notation). The density of states for these parameters (see figure 1 of [6]) has a pronounced peak for the particle-density $n_\sigma \approx 0.3$. For this band-filling we observe the strongest tendency to generate a ferromagnetic order, in qualitative agreement with the simple Stoner criterion. Therefore, we consider the spin-wave properties of our system only for this optimum band-filling. The numerical

evaluation in [6] did not respect the global spin-symmetry of the wave-function $|\Psi_G\rangle$. In this work, we include the additional constraints on the variational-parameters λ_Γ as described in appendix A, and we obtain almost the same state as in [6]. In other words, in the two-band-model even the general variational ground-state $|\Psi_G\rangle$, as defined in (7), is a nearly perfect eigenstate of the global spin-operator. However, it is not clear so far, if this statement also holds for a more general multi-band model.

In [6] we found significant differences between the Hartree–Fock and the Gutzwiller theory. These differences have to be interpreted as a failure of the Hartree–Fock theory since the variational space of the Hartree–Fock theory is included in our general class of Gutzwiller wave-functions. Although this statements holds for the corresponding RPA-theory as well, this theory is generally considered as the standard method in the context of spin-waves in itinerant ferromagnets [12].

The ferromagnetic phase diagram for our model is shown in figure 2. In the Hartree–Fock theory ferromagnetism occurs for considerably smaller values of the correlation parameters. The most important difference lies in the role of the interatomic exchange J. In the Gutzwiller theory a ferromagnetic ground-state exists only for finite values of J. This is completely different in the Hartree–Fock theory. There, the only relevant quantities are the Stoner-parameter $I = (U + J)/2$ and the density of states at the Fermi-level $\mathfrak{D}_0(E_F)$ which enter the Stoner criterion

$$I\mathfrak{D}_0(E_F) > 1. \tag{57}$$

This means that even for $J = 0$ finite values of U exist, where the system makes a transition into a ferromagnetic state.

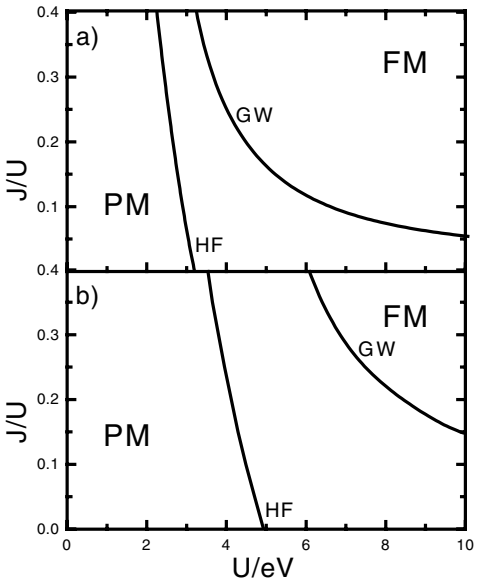

Figure 2. Phase diagram as a function of U and J for the Hartree–Fock–Stoner theory (HF) and the Gutzwiller wave function (GW) for (a) $n_\sigma = 0.29$ and (b) $n_\sigma = 0.35$; PM: paramagnet, FM: ferromagnet.

Another important difference between both theories occurs when we compare the condensation energies E_{cond}, i.e., the differences between the energies in the paramagnetic and the ferromagnetic ground states. This quantity should have the same order of magnitude as the Curie-temperature T_C in itinerant ferromagnets. In Stoner theory we observe that E_{cond} is typically of the order of U and therefore much larger than T_C. This is in agreement with the general observation that mean field methods overestimate the stability of magnetic order.

On the other hand, in our correlated electron approach we find relatively small values for the condensation energy even for interaction parameters as large as twice the bandwidth.

5.2. Spin-waves

Figure 3 shows the spin-wave dispersion in the (100) direction for four different magnetizations. As the lattice constant of our simple-cubic lattice we chose $a = 2.5$ Å, the next-neighbour distance in nickel. Our Gutzwiller theory shows that the dispersion strongly depends on the magnetization, especially for small values of $\vec{q}$. The line shows the respective fits for the function

$$E_{\vec{q}} = Dq^2(1 - \beta q^2). \tag{58}$$

Note that experimental results of the region where quartic corrections become dominant are usually not very accurate, since Stoner excitations reduce the lifetime of spin-waves significantly. The values for the spin-wave stiffness $D = 1.4$ eV Å^2 and $D = 1.2$ eV Å^2 in both cases of almost fully polarized magnetizations, $m = 0.26$ and $m = 0.28$, respectively, are of the right order of magnitude for nickel where $D = 0.43$ eV Å^2.

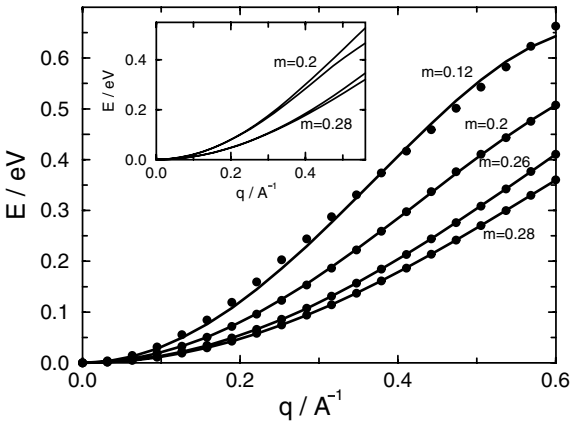

Figure 3. Variational spin wave dispersion in the (100) direction, for the two-band model; $n_\sigma = 0.29$, $J = 0.2U$, and the values $U/\text{eV} = 7.8, 10, 12, 13.6$ correspond to $m = 0.12, 0.20, 0.26, 0.28$; Inset: variational spin wave dispersion in (100) and (110) direction; $n_\sigma = 0.29$, $J = 0.2U$, and the values $U/\text{eV} = 10, 13.6$ correspond to $m = 0.2, 0.28$.

The spin-wave dispersion is almost isotropic, as can be seen for example in the inset of figure 3, where the dispersion is shown in the directions (100) and (110). Such isotropic behaviour was also observed in experiments on iron and nickel and it is actually somewhat surprising, since the band-structure in these materials is far from being isotropic. However, we should bear in mind that even in a metallic system local moments are formed due to the electrons' correlations. Therefore, spin-excitations may be interpreted as spin-fluctuations in a system with localized spins. In such a system we have a generic isotropy when the exchange coupling is dominated by terms between nearest-neighbours.

Our results show that the magnetic excitations in strong itinerant ferromagnets behave very similarly to those in systems of localized spins. These low-energy excitations are responsible for the magnetic phase transition which occurs for temperatures much smaller than the typical Fermi energies in itinerant electron systems. This observation is consistent with the small

condensation energy in our variational approach. To support this statement let us consider a Heisenberg-model

$$\hat{H}_S = -J \sum_{\langle i,j \rangle} \vec{S}_i \vec{S}_j$$

on a cubic lattice. In this system we have a spin-wave stiffness $D = 2SJa^2$. The value of the effective local moment in our itinerant system is given as $S \approx 0.6$ (see [6]). Therefore we obtain $J = D/2Sa^2 \approx 0.16$ eV. For an estimate of the Curie temperature we use the results from quantum Monte-Carlo calculations $T_C = 1.44\, JS^2$ [23]. In this way we find $T_C \approx 8 \times 10^2$ K which is the same order of magnitude as the condensation energy $E_{\mathrm{cond}} \approx 5 \times 10^2$ K. Thus, we can summarize that our variational approach gives a consistent picture of both of magnetic excitations and ground-state properties in strong itinerant ferromagnets.

When the spin-waves are treated as non-interacting bosons, their contribution to the specific heat and the magnetization $M(T)$ may be calculated from $E_{\vec{q}}$. The first-order contribution stems from the quadratic term and is the well known $T^{3/2}$-law [24]. The next order depends on the behaviour of $E_{\vec{q}}$ for larger values of q. It is still not clear, whether or not the quartic term in (58) describes the generic feature in the experiments. Some experiments indicate that the second term in $M(T)$ is αT^2, which could be explained with a linear behaviour in $E_{\vec{q}}$. Our dispersion $E_{\vec{q}}$ also allows us to calculate such temperature-dependent quantities numerically. However, we did not analyse this for our two-band model, because these results could not be compared to experiments.

6. Summary and conclusion

In this paper we presented a variational method for the description of spin-wave excitations in itinerant ferromagnets. Our starting point was a general multi-band Hubbard-model which is an appropriate model for elements of the iron group. Earlier work showed that ferromagnetism in metals requires substantial interaction strengths even in systems with orbital degeneracy. Therefore, we suspect that weak-coupling theories are not able to describe the physics of itinerant ferromagnets correctly. Our method is based on a variational study of multi-band Hubbard models with the help of generalized Gutzwiller wave functions. These wave functions yield the exact ground-state both in the uncorrelated and the atomic limit of the Hubbard model. Therefore, we expect them to describe reasonably the ground-state properties for finite values of the correlation parameters.

From a theoretical point of view, spin waves are given as peaks in the imaginary part $\chi_T(\vec{q}, E)$ of the transversal spin susceptibility. This quantity can be measured using inelastic neutron scattering. For $\vec{q} = \vec{0}$ the spin-symmetry of the ferromagnetic ground-state leads to an isolated peak $\delta(E)$ in χ_T. We assume that this peak is broadened only moderately for finite values of $\vec{q}$. Then, the position of the peak, which is interpreted as the spin-wave dispersion $E_{\vec{q}}$, can be calculated as a static expectation-value of spin-operators in the ground state of the system. In our approximation we use the variational instead of the true ground state and calculate all expectation values in the limit of large spatial dimensions.

Our results may be evaluated numerically for general multi-band models to describe iron and nickel. However, the main numerical problem is the determination of the optimum variational wave-function for these realistic systems with a non-trivial atomic Hamiltonian. Work in this direction is still in progress. In this work we applied our method to a two-band model. Here, we found a behaviour which is in qualitative agreement with experimental results for strong ferromagnets. The spin-wave dispersion $E_{\vec{q}}$ is almost isotropic and quadratic for small values of $\vec{q}$. For larger $\vec{q}$ we found quartic corrections, which are also seen in some of the

experiments. The values of the spin-wave stiffness have the right order of magnitude compared to experiments. We concluded that the low-lying magnetic excitations in our correlated and itinerant electron system are similar to those in a localized spin system. When we estimate the Curie-temperature T_C from our spin-wave properties and compare it to the condensation energy we find a consistent picture in our variational approach. The ferromagnetic phase transition is driven by spin-waves and the value for T_C is therefore much smaller than typical Fermi energies in itinerant electron systems.

Acknowledgment

The author is very grateful to F Gebhard and R Thul for a critical reading of the manuscript and many helpful discussions.

Appendix A. Global spin-symmetry

The variational spin-wave dispersion (25) is gapless only if the variational wave-function $|\Psi_G\rangle$ is an eigenstate of the global spin-operators (30). This symmetry is not fulfilled for an arbitrary choice of the variational parameters λ_Γ in (8). In this appendix, we present two ways to implement this symmetry.

The first way to guarantee the global spin symmetry of $|\Psi_G\rangle$ starts from the fact that the one-particle product-state $|\Phi_0\rangle$ in (7) may in general be chosen as an eigenstate both of $\hat{\vec{S}}^2$ and $\hat{S}^z$. In this case, $|\Psi_G\rangle$ is an eigenstate of $\hat{S}^z$ if the states $|\Gamma\rangle$ are chosen as eigenstates of the local spin-operator in z direction. Then, the correct spin-symmetry of $|\Psi_G\rangle$ is ensured if $|\Psi_G\rangle$ is an eigenstate of $\hat{S}^+\hat{S}^-$. It is equivalent to demand that

$$\langle \hat{S}^+\hat{S}^- \rangle_{\Psi_G} = 2S_z \tag{A1}$$

since we may assume that the spin in $|\Psi_G\rangle$ has a maximal component in z direction. The left-hand-side of equation (A1) is just the norm $N_{\vec{q}}$ for $\vec{q} \to \vec{0}$ which was derived in (55*a*). Thus, (A1) together with (55*a*) leads to *one* additional condition for the variational parameters λ_Γ. However, this condition is not very helpful, because equation (55*a*) includes the optimum values λ_Γ. This means that (A1) has to be included in the minimization algorithm, which determines the optimum wave-function $|\Psi_G\rangle$; numerically, this is a very difficult problem.

In the following we propose a second, more feasible strategy for the implementation of the correct spin-symmetry. To this end, we arrange the orbitals on the atoms of our system into groups which carry the index of the respective representation D of the point-symmetry group. Then, we define the operators

$$\hat{N}^s_D = \sum_{i,b\in D} \hat{n}_{i;(bs)} \qquad \hat{M}^s_D = \sum_{i,b\in D} \hat{m}_{i;(bs)} \tag{A2}$$

for the gross and net number of electrons in orbitals of the representation D and with spin s. Again, we assume that each representation occurs only once. Under this condition, group theoretical arguments show that the following relation holds

$$\sum_{b\in D} \hat{m}_{i;(bs)} = \sum_{b\in D} \hat{n}_{i;(bs)} - \sum_{\Gamma(|\Gamma|\geqslant 2)} f^s_D(\Gamma)\hat{m}_{i;\Gamma} \tag{A3}$$

where

$$f^s_D(\Gamma) = \sum_{b\in D} \sum_{I((b,s)\notin I)} \left| T_{\Gamma, I\cup(b,s)} \right|^2 . \tag{A4}$$

Thus, we can write

$$\hat{M}_D^s = \hat{N}_D^s - \sum_{\Gamma(|\Gamma|\geqslant 2)} f_D^s(\Gamma)\hat{M}_\Gamma \tag{A5a}$$

$$\hat{M}_\Gamma \equiv \sum_i \hat{m}_{i;\Gamma} \tag{A5b}$$

and the Gutzwiller-projector (8) becomes

$$\hat{P}_G = \prod_{D,s} \left(\lambda_D^s\right)^{\hat{N}_D^s} \prod_\Gamma \tilde{\lambda}_\Gamma^{\hat{M}_\Gamma}. \tag{A6}$$

Here, we already assumed that the parameters $\lambda_{(b,s)} (\equiv \lambda_D^s)$ are the same for all orbitals, which belong to D. Further, we introduced

$$\tilde{\lambda}_\Gamma = \lambda_\Gamma \prod_{D,s} \left(\lambda_D^s\right)^{-f_D^s(\Gamma)}. \tag{A7}$$

Now, we postulate the following conditions which ensure that $|\Psi_G\rangle$ is an eigenstate of the operator $\hat{\vec{S}}^2$:

(i) $\lambda_D^s = \lambda_{D'}^s \equiv \lambda_s$ for all representations D, D',

(ii) $\tilde{\lambda}_{\Gamma_S^{S_z}} = \tilde{\lambda}_{\Gamma_S^{S_z'}} \equiv \tilde{\lambda}_{\Gamma_S}$ for all states $\left|\Gamma_S^{S_z}\right\rangle$, $\left|\Gamma_S^{S_z'}\right\rangle$, which belong to the same spin-multiplet $(\equiv \Gamma^S)$ with spin S.

For the proof of this statement, we can first conclude from (i) that the state $|\Phi_0\rangle$ is an eigenstate of

$$\prod_{D,s} \left(\lambda_D^s\right)^{\hat{N}_D^s} = \prod_s \lambda_s^{\hat{N}_s} \tag{A8}$$

where $\hat{N}_s = \sum_D \hat{N}_D^s$ is the number-operator for electrons with spin s. Thus, we have

$$\hat{S}^+\hat{S}^-|\Psi_G\rangle = \hat{S}^+\hat{S}^- \prod_s \lambda_s^{\hat{N}_s} \prod_\Gamma \tilde{\lambda}_\Gamma^{\hat{M}_\Gamma}|\Phi_0\rangle \tag{A9a}$$

$$\sim \hat{S}^+\hat{S}^- \prod_\Gamma \tilde{\lambda}_\Gamma^{\hat{M}_\Gamma}|\Phi_0\rangle \tag{A9b}$$

since $\left[\hat{N}_s, \hat{M}_\Gamma\right] = 0$ for all s, Γ. We introduce the operator

$$\hat{M}_{\Gamma_S} \equiv \sum_{S_z=-S}^{S} \hat{M}_{\Gamma_S^{S_z}} \tag{A10}$$

which has the property $\left[\hat{S}^\pm, \hat{M}_{\Gamma_S}\right] = 0$. Then, condition (ii) finally gives

$$\hat{S}^+\hat{S}^-|\Psi_G\rangle \sim \hat{S}^+\hat{S}^- \prod_{\Gamma_S} \tilde{\lambda}_{\Gamma_S}^{\hat{M}_{\Gamma S}}|\Phi_0\rangle \sim \prod_{\Gamma^S} \tilde{\lambda}_{\Gamma_S}^{\hat{M}_{\Gamma_S}} \hat{S}^+\hat{S}^-|\Phi_0\rangle \sim |\Psi_G\rangle \tag{A11}$$

such that $|\Psi_G\rangle$ is an eigenstate of $\hat{\vec{S}}^2$.

Note, that condition (ii) reduces the number of variational parameters significantly, since all parameters λ_Γ for states $|\Gamma\rangle$, which belong to the same spin-multiplet Γ_S are now determined by just one parameter $\tilde{\lambda}_{\Gamma_S}$. However, this restriction still allows different occupations of the several S_z components, since

$$m_{\Gamma_S^{S_z}} = \lambda_{\Gamma_S} m^0_{\Gamma_S^{S_z}} \tag{A12}$$

also depends on the one-particle-state $|\Phi_0\rangle$.

The one-particle-occupations

$$m_{(bs)} = \lambda_{(bs)} m^0_{(bs)} = \lambda_s m^0_{(bs)} \equiv m^s_D \tag{A13}$$

with $b \in D$ depend on the quantities $n^s_D \equiv n_{(bs)}$ and $\mathrm{m}_{\Gamma_S^{S_z}}$ (see equation (A3)),

$$m^s_D = n^s_D - \sum_{\Gamma_S(|\Gamma_S| \geqslant 2)} \sum_{S_z=-S}^{S} f^s_D(\Gamma_S^{S_z}) m_{\Gamma_S^{S_z}}. \tag{A14}$$

However, the additional conditions (i) and (ii) prevent us from deriving an analytical expression for m^s_D, since the parameters $m_{\Gamma_S^{S_z}}$ depend on m^s_D via (A7) and (A12). Therefore, the relation (A14) has to be implemented into our minimization algorithm with the help of appropriate Lagrange parameters.

Appendix B. Diagrams and vertices

Appendix B.1. The vertices $\tilde{x}^{\mathfrak{D}'}_{\mathfrak{D}}$ and $\tilde{\xi}^{\mathfrak{D}'\mathfrak{D}''}_{\mathfrak{D}}$

In section 4 the vertices $\tilde{x}^{\mathfrak{D}'}_{\mathfrak{D}}$ (see equations (42) and (44)) have been derived in terms of the coefficients $x_{II'}$, which occur in the expansion (10). Now we will derive an explicit expression for these coefficients. The operator (50*b*) may be written as

$$m^{I_1,I_2}_{J'} = \prod_{\sigma \in J'} \left(n^0_\sigma + \hat{n}^{\mathrm{HF}}_\sigma \right) \prod_{\sigma \in \bar{J}' \setminus (I_1 \cup I_2)} \left(1 - n^0_\sigma - \hat{n}^{\mathrm{HF}}_\sigma \right) \tag{B1}$$

$$= \sum_{J(I_1,I_2 \notin J)} \left[(-1)^{|J \cap \bar{J}'|} \prod_{\sigma \in J' \setminus J} n^0_\sigma \prod_{\sigma \in \bar{J}' \setminus \{J \cup I_1 \cup I_2\}} (1 - n^0_\sigma) \right] \hat{n}^{\mathrm{HF}}_J \tag{B2}$$

where $I_1, I_2 \notin J$ means that $J \cap (I_1 \cup I_2) = \emptyset$. Thus, $\hat{P}^2_G$ becomes

$$\hat{P}^2_G = 1 + \sum_\Gamma (\lambda^2_\Gamma - 1) \sum_{I_1,I_2(I_1 \cap I_2 = \emptyset)} \sum_{J'(I_1,I_2 \notin J')} T_{J' \cup I_1,\Gamma} T^+_{\Gamma,J' \cup I_2} f^{J'}_{I_1} f^{J'}_{I_2} \left(\prod_{\sigma \in I_1 \cup I_2} \frac{1}{1 - n^0_\sigma} \right)$$

$$\times \sum_{J(I_1,I_2 \notin J)} \left[(-1)^{|J \cap \bar{J}'|} \prod_{\sigma \in J' \setminus J} n^0_\sigma \prod_{\sigma \in \bar{J}' \setminus J} (1 - n^0_\sigma) \right] \hat{n}^{HF}_{J \cup I_1, J \cup I_2}. \tag{B3}$$

A comparison of the coefficients in (B3) and (10) gives

$$x_{J \cup I_1, J \cup I_2} = \sum_\Gamma (\lambda^2_\Gamma - 1) \sum_{J'(I_1,I_2 \notin J')} T_{J' \cup I_1,\Gamma} T^+_{\Gamma,J' \cup I_2} f^{J'}_{I_1} f^{J'}_{I_2} \left(\prod_{\sigma \in I_1 \cup I_2} \frac{1}{1 - n^0_\sigma} \right)$$

$$\times \left[(-1)^{|J \cap \bar{J}'|} \prod_{\sigma \in J' \setminus J} n^0_\sigma \prod_{\sigma \in \bar{J}' \setminus J} (1 - n^0_\sigma) \right]. \tag{B4}$$

In appendix C we need an expression for vertices

$$\tilde{\xi}^{\mathfrak{D}'\mathfrak{D}''}_{\mathfrak{D}} = \tilde{\xi}^{(\sigma_3\sigma_4)(\sigma_5\sigma_6)}_{(\sigma_1\sigma_2)} \tag{B5}$$

with three incoming and outgoing lines, which stem from a term like

$$y_{l;(\sigma_1,\sigma_3,\sigma_5)(\sigma_2,\sigma_4,\sigma_6)} \left\{ \ldots \left(\hat{c}^+_{l,\sigma_1} \hat{c}_{l,\sigma_2} \right) \left(\hat{c}^+_{l,\sigma_3} \hat{c}_{l,\sigma_4} \right) \left(\hat{c}^+_{l,\sigma_5} \hat{c}_{l,\sigma_6} \right) \ldots \right\}^c_{\Phi_0} f^{\sigma_3}_{\sigma_1} f^{\sigma_1 \cup \sigma_3}_{\sigma_5} f^{\sigma_4}_{\sigma_2} f^{\sigma_2 \cup \sigma_4}_{\sigma_6} \tag{B6}$$

where $y_{l;I,I'}$ can be determined from equation (42). Hence, the vertices (B5) are given as

$$\tilde{\xi}^{(\sigma_3\sigma_4)(\sigma_5\sigma_6)}_{(\sigma_1\sigma_2)} = f^{\sigma_3}_{\sigma_1} f^{\sigma_1 \cup \sigma_3}_{\sigma_5} f^{\sigma_4}_{\sigma_2} f^{\sigma_2 \cup \sigma_4}_{\sigma_6} x_{(\sigma_1,\sigma_3,\sigma_5)(\sigma_2,\sigma_4,\sigma_6)}. \tag{B7}$$

Appendix B.2. Diagrams

In appendices C and D we need some diagrams, which can be evaluated in momentum-space as follows:
(1)

$$W^{(\sigma_1\sigma_2)}_{(\sigma_3\sigma_4)(\sigma_5\sigma_6)}(\vec{q}) \equiv \sum_{i\neq j\neq l} \mathrm{e}^{\mathrm{i}\vec{q}(\vec{R}_j-\vec{R}_l)} P^{\sigma_1\sigma_4}_{i,j} P^{\sigma_3\sigma_6}_{j,l} P^{\sigma_5\sigma_2}_{l,i} \tag{B8a}$$

$$= \sum_{\vec{k}} n^{\sigma_1\sigma_4}_{\vec{k}} n^{\sigma_3\sigma_6}_{\vec{k}+\vec{q}} n^{\sigma_5\sigma_2}_{\vec{k}} - \delta^{\sigma_6}_{\sigma_3} n^0_{\sigma_3} \tilde{P}^{(\sigma_1\sigma_2)}_{(\sigma_5\sigma_4)}(\vec{0}) - \delta^{\sigma_5}_{\sigma_2} n^0_{\sigma_2} \tilde{P}^{(\sigma_1\sigma_6)}_{(\sigma_3\sigma_4)}(\vec{q})$$

$$-\delta^{\sigma_4}_{\sigma_1} n^0_{\sigma_1} \tilde{P}^{(\sigma_3\sigma_2)}_{(\sigma_5\sigma_6)}(\vec{q}) + 2\delta^{\sigma_4}_{\sigma_1}\delta^{\sigma_6}_{\sigma_3}\delta^{\sigma_5}_{\sigma_2} n^0_{\sigma_1} n^0_{\sigma_2} n^0_{\sigma_3} \tag{B8b}$$

(2)

$$E^{(\sigma_3\sigma_4)}_{(\sigma_1\sigma_2)}(\vec{q}) \equiv \sum_{i,j} \mathrm{e}^{\mathrm{i}\vec{q}(\vec{R}_i-\vec{R}_j)} t^{\sigma_3\sigma_4}_{i,j} P^{\sigma_1\sigma_2}_{i,j} = \sum_{\vec{k}} \varepsilon^{\sigma_3\sigma_4}_{\vec{k}} n^{\sigma_1\sigma_2}_{\vec{k}+\vec{q}} \tag{B9}$$

with

$$\varepsilon^{\sigma_3\sigma_4}_{\vec{k}} \equiv \frac{1}{L} \sum_{i,j} \mathrm{e}^{i\vec{k}(\vec{R}_i-\vec{R}_j)} t^{\sigma_3\sigma_4}_{i,j} \tag{B10}$$

(3)

$$V^{(\sigma_1\sigma_2)}_{(\sigma_3\sigma_4)(\sigma_5\sigma_6)}(\vec{q}) \equiv -\sum_{i\neq j\neq l} \mathrm{e}^{\mathrm{i}\vec{q}(\vec{R}_i-\vec{R}_l)} t^{\sigma_5\sigma_6}_{i,j} P^{\sigma_3\sigma_2}_{i,l} P^{\sigma_1\sigma_4}_{l,j} \tag{B11a}$$

$$= -\sum_{\vec{k}} \varepsilon^{\sigma_5\sigma_6}_{\vec{k}} n^{\sigma_3\sigma_2}_{\vec{k}+\vec{q}} n^{\sigma_1\sigma_4}_{\vec{k}} + \delta^{\sigma_3}_{\sigma_2} n^0_{\sigma_2} E^{(\sigma_5\sigma_6)}_{(\sigma_1\sigma_4)}(\vec{0}) + \delta^{\sigma_4}_{\sigma_1} n^0_{\sigma_1} E^{(\sigma_5\sigma_6)}_{(\sigma_3\sigma_2)}(\vec{q}) \tag{B11b}$$

and

$$\bar{V}^{(\sigma_1\sigma_2)}_{(\sigma_3\sigma_4)(\sigma_5\sigma_6)}(\vec{q}) \equiv -\sum_{i\neq j\neq l} \mathrm{e}^{i\vec{q}(\vec{R}_l-\vec{R}_j)} t^{\sigma_5\sigma_6}_{i,j} P^{\sigma_3\sigma_2}_{i,l} P^{\sigma_1\sigma_4}_{l,j} \tag{B12a}$$

$$= -\sum_{\vec{k}} \varepsilon^{\sigma_5\sigma_6}_{\vec{k}} n^{\sigma_3\sigma_2}_{\vec{k}} n^{\sigma_1\sigma_4}_{\vec{k}+\vec{q}} + \delta^{\sigma_3}_{\sigma_2} n^0_{\sigma_2} E^{(\sigma_5\sigma_6)}_{(\sigma_1\sigma_4)}(\vec{q}) + \delta^{\sigma_4}_{\sigma_1} n^0_{\sigma_1} E^{(\sigma_5\sigma_6)}_{(\sigma_3\sigma_2)}(\vec{0}) \tag{B12b}$$

(4)

$$U^{(\sigma_1\sigma_2)}_{(\sigma_3\sigma_4)(\sigma_5\sigma_6)}(\vec{q}) \equiv \sum_{i\neq j\neq l\neq m} \mathrm{e}^{i\vec{q}(\vec{R}_m-\vec{R}_l)} t^{\sigma_1\sigma_2}_{i,j} P^{\sigma_1\sigma_4}_{i,m} P^{\sigma_3\sigma_6}_{m,l} P^{\sigma_5\sigma_2}_{l,j} \tag{B13a}$$

$$= \sum_{\vec{k}} \varepsilon^{\sigma_1\sigma_2}_{\vec{k}} n^{\sigma_1\sigma_4}_{\vec{k}} n^{\sigma_3\sigma_6}_{\vec{k}+\vec{q}} n^{\sigma_5\sigma_2}_{\vec{k}} - \delta^{\sigma_6}_{\sigma_3} n^0_{\sigma_3} V^{(\sigma_5\sigma_4)}_{(\sigma_1\sigma_2)(\sigma_1\sigma_2)}(\vec{0})$$

$$-\delta^{\sigma_4}_{\sigma_1} n^0_{\sigma_1} V^{(\sigma_5\sigma_6)}_{(\sigma_3\sigma_2)(\sigma_1\sigma_2)}(\vec{q}) - \delta^{\sigma_5}_{\sigma_2} n^0_{\sigma_2} \bar{V}^{(\sigma_3\sigma_4)}_{(\sigma_1\sigma_6)(\sigma_1\sigma_2)}(\vec{q})$$

$$-\delta^{\sigma_4}_{\sigma_1}\delta^{\sigma_5}_{\sigma_2} n^0_{\sigma_1} n^0_{\sigma_2} E^{(\sigma_1\sigma_2)}_{(\sigma_3\sigma_6)}(\vec{q}) - \delta^{\sigma_4}_{\sigma_1}\delta^{\sigma_6}_{\sigma_3} n^0_{\sigma_1} n^0_{\sigma_3} E^{(\sigma_1\sigma_2)}_{(\sigma_5\sigma_2)}(\vec{0})$$

$$-\delta^{\sigma_5}_{\sigma_2}\delta^{\sigma_6}_{\sigma_3} n^0_{\sigma_1} n^0_{\sigma_3} E^{(\sigma_1\sigma_2)}_{(\sigma_1\sigma_4)}(\vec{0}) - \tilde{P}^{(\sigma_1\sigma_6)}_{(\sigma_3\sigma_4)}(\vec{q}) E^{(\sigma_1\sigma_2)}_{(\sigma_5\sigma_2)}(\vec{q})$$

$$-\tilde{P}^{(\sigma_5\sigma_6)}_{(\sigma_3\sigma_2)}(\vec{q}) E^{(\sigma_1\sigma_2)}_{(\sigma_1\sigma_4)}(\vec{q}). \tag{B13b}$$

Appendix C. Evaluation of the atomic interaction

According to equation (28*a*) we have to analyse the expectation values

$$\frac{1}{N_{\vec{q}}}\sum_k \langle \Psi_{\vec{q}}^G | \hat{m}_{k;\Gamma} | \Psi_{\vec{q}}^G \rangle = \frac{1}{N_{\vec{q}}}\sum_{i,j,k} \mathrm{e}^{\mathrm{i}\vec{q}(\vec{R}_i-\vec{R}_j)} \langle \Psi_G | \hat{S}_i^+ \hat{m}_{k;\Gamma} \hat{S}_j^- | \Psi_G \rangle \tag{C1a}$$

$$= \frac{1}{N_{\vec{q}}}\sum_k \Bigg[\sum_{i,j(\neq k)} \mathrm{e}^{\mathrm{i}\vec{q}(\vec{R}_i-\vec{R}_j)} \langle \Psi_G | \hat{S}_i^+ \hat{S}_j^- \hat{m}_{k;\Gamma} | \Psi_G \rangle \tag{C1b}$$

$$+ \sum_{j(\neq k)} \Big(\mathrm{e}^{\mathrm{i}\vec{q}(\vec{R}_k-\vec{R}_j)} \langle \Psi_G | \hat{S}_k^+ \hat{m}_{k;\Gamma} \hat{S}_j^- | \Psi_G \rangle + \text{c.c.} \Big) \tag{C1c}$$

$$+ \langle \Psi_G | \hat{S}_k^+ \hat{m}_{k;\Gamma} \hat{S}_k^- | \Psi_G \rangle \Bigg] \tag{C1d}$$

This evaluation will be done separately for the three terms (C1*b*)–(C1*d*).

In the first term (C1*b*), we have to distinguish connected and unconnected diagrams. Here, the term 'connected' means, that the lattice site k is connected to one of the lattice sites i, j. This condition necessarily requires that k is connected to both lattice sites i and j, because $\hat{S}_i^+$ or $\hat{S}_j^-$ generate a spin-flip. Such a process cannot be compensated in a diagram with only one of these operators, either by the external vertex-operator $\hat{m}_{k;\Gamma}$ or by one of the internal vertex-operators $\hat{n}^{HF}_{l;I,I'}$.

The unconnected terms can be written as

$$(C1b)^{uc} = \frac{1}{N_{\vec{q}}}\sum_k \frac{\langle \Psi_G | \hat{m}_{k;\Gamma} | \Psi_G \rangle}{N_G} \times \Bigg[\sum_{i\neq j(\neq k)} \mathrm{e}^{\mathrm{i}\vec{q}(\vec{R}_i-\vec{R}_j)} \Big\langle \big(\hat{P}_{i;G}\hat{S}_i^+\hat{P}_{i;G}\big)\big(\hat{P}_{j;G}\hat{S}_j^-\hat{P}_{j;G}\big) \prod_{l(\neq i,j,k)} \hat{P}^2_{l;G} \Big\rangle_{\Phi_0} + \sum_i \Big\langle \big(\hat{P}_{i;G}\hat{S}_i^+\hat{S}_i^-\hat{P}_{i;G}\big) \prod_{l(\neq i,k)} \hat{P}^2_{l;G} \Big\rangle_{\Phi_0} \Bigg]. \tag{C2}$$

When we ignore the restriction $i, j, l \neq k$, the sum over i and j gives just $N_{\vec{q}}$. Thus, we find the correct result for $(\mathrm{C1}b)^{\mathrm{uc}}$ by substracting all diagrams with $i = k$ or $j = k$ for an external vertex, or $l = k$ for one of the internal vertices. These contributions are given as

$$\begin{array}{lcl} i = j = k & : & N_{\mathrm{G}} \sum_{\Gamma'} S_-(\Gamma') m_{\Gamma'} \\ i = k \text{ or } j = k & : & 2N_{\mathrm{G}} \vec{S}^+ \cdot \tilde{\Omega}(\vec{q}\,) \cdot \vec{S}^- \\ l = k & : & N_{\mathrm{G}} \vec{S}^+ \cdot \tilde{\Omega}(\vec{q}\,) \cdot \tilde{x} \cdot \tilde{\Omega}(\vec{q}\,) \cdot \vec{S}^- \,. \end{array}$$

Altogether, we obtain the following expression for the contribution of the unconnected diagrams:

$$(C1b)^{\mathrm{uc}} = \Bigg[L m_\Gamma - m_\Gamma \frac{L N_G}{N_{\vec{q}}} \Big(2\vec{S}^+ \cdot \tilde{\Omega}(\vec{q}) \cdot \vec{S}^- + \sum_{\Gamma'} S_-(\Gamma') m_{\Gamma'} + \vec{S}^+ \cdot \tilde{\Omega}(\vec{q}) \cdot \tilde{x} \cdot \tilde{\Omega}(\vec{q}) \cdot \vec{S}^- \Big) \Bigg] \tag{C3a}$$

$$\equiv L m_\Gamma + m_\Gamma^1(\vec{q}), \tag{C3b}$$

where $LN_{\rm G}/N_{\vec{q}}$ is given in (55a). Note that only the second term $m^1_\Gamma(\vec{q})$ is relevant for our spin-wave-dispersion $E^{var}_{\vec{q}}$, since the first term Lm_Γ is cancelled by the respective ground-state contribution in equation (25).

For the connected diagrams in (C1b) we may distinguish between those diagrams with two or four lines, which enter or leave the external vertex. The vertex-factors with two lines can be evaluated from (51), whereas the respective factor with four lines stems from the expansion

$$\left\{\ldots \hat{m}_{I_1,I_2}\ldots\right\}^C_{\Phi_0} \rightarrow \sum_{\sigma_1,\sigma_2,\sigma_3,\sigma_4} \tilde{\mathfrak{V}}^{(\sigma_1\sigma_2)(\sigma_3\sigma_4)}_{I_1,I_2} \left\{\ldots \left(\hat{c}^+_{\sigma_1}\hat{c}_{\sigma_2}\right)\left(\hat{c}^+_{\sigma_3}\hat{c}_{\sigma_4}\right)\ldots\right\}^c_{\Phi_0} \tag{C4}$$

$$\begin{aligned}\tilde{\mathfrak{V}}^{(\sigma_1\sigma_2)(\sigma_3\sigma_4)}_{I_1,I_2} = &\sum_{J(\sigma_1,\sigma_2,\sigma_3,\sigma_4\notin J)} f^J_{\sigma_1} f^J_{\sigma_2} f^J_{\sigma_3} f^J_{\sigma_4} m^0_J \left(\prod_{\sigma\in(\sigma_1,\sigma_2,\sigma_3,\sigma_4)} \frac{1}{(1-n^0_\sigma)}\right)\\ &\times\Big[f^{\sigma_3}_{\sigma_1} f^{\sigma_4}_{\sigma_2}\delta^{I_1}_{J\cup(\sigma_1,\sigma_3)}\delta^{I_2}_{J\cup(\sigma_2,\sigma_4)} - \delta^{\sigma_2}_{\sigma_1}\delta^{I_1}_{J\cup\sigma_3}\delta^{I_2}_{J\cup\sigma_4} - \delta^{\sigma_4}_{\sigma_3}\delta^{I_1}_{J\cup\sigma_1}\delta^{I_2}_{J\cup\sigma_2}\\ &+\delta^{\sigma_4}_{\sigma_1}\delta^{I_1}_{J\cup\sigma_3}\delta^{I_2}_{J\cup\sigma_2} + \delta^{\sigma_3}_{\sigma_2}\delta^{I_1}_{J\cup\sigma_1}\delta^{I_2}_{J\cup\sigma_4} + (\delta^{\sigma_2}_{\sigma_1}\delta^{\sigma_4}_{\sigma_3} - \delta^{\sigma_4}_{\sigma_1}\delta^{\sigma_3}_{\sigma_2})\delta^{I_1}_J\delta^{I_2}_J\Big]\end{aligned} \tag{C5}$$

which is also derived for $|I_1| = |I_2|$. This expression together with equation (49) leads to the following external vertex $\overset{+}{T}{}^{\mathfrak{D}'}_{\mathfrak{D}}$ for the operator $\hat{S}^+_i$

$$\overset{+}{T}{}^{(\sigma_3\sigma_4)}_{(\sigma_1\sigma_2)} = \sum_\Gamma \lambda_{\Gamma_+}\lambda_\Gamma\sqrt{S_+(\Gamma)}\sum_{I_1,I_2} T_{I_1,\Gamma_+}T^+_{\Gamma,I_2}\tilde{\mathfrak{V}}^{(\sigma_1\sigma_2)(\sigma_3\sigma_4)}_{I_1,I_2} \tag{C6}$$

whereas the corresponding factor $\overset{-}{T}{}^{\mathfrak{D}'}_{\mathfrak{D}}$ for the operator $\hat{S}^-_j$ is given as

$$\overset{-}{T}{}^{(\sigma_3\sigma_4)}_{(\sigma_1\sigma_2)} = \left(\overset{+}{T}{}^{(\sigma_4\sigma_3)}_{(\sigma_2\sigma_1)}\right)^*. \tag{C7}$$

Using equations (51), (C4), and

$$\hat{P}_G\hat{m}_\Gamma\hat{P}_G = \sum_{I_1,I_2}\lambda^2_\Gamma T_{I_1,\Gamma}T^+_{I_2,\Gamma}\hat{m}_{I_1,I_2} \tag{C8}$$

we obtain the following expression for the vertices of the external-operator in (C1b) with one or two incoming and outgoing lines,

$$M_{(\sigma_1\sigma_2)}(\Gamma) = \sum_{I_1,I_2}\lambda^2_\Gamma T_{I_1,\Gamma}T^+_{I_2,\Gamma}\mathfrak{V}^{(\sigma_1\sigma_2)}_{I_1,I_2} \tag{C9a}$$

$$\tilde{M}^{(\sigma_3\sigma_4)}_{(\sigma_1\sigma_2)}(\Gamma) = \sum_{I_1,I_2}\lambda^2_\Gamma T_{I_1,\Gamma}T^+_{I_2,\Gamma}\tilde{\mathfrak{V}}^{(\sigma_1\sigma_2)(\sigma_3\sigma_4)}_{I_1,I_2}. \tag{C9b}$$

When we define the vector $\vec{M}(\Gamma)$ of components $M_{\mathfrak{D}}(\Gamma)$, we may write the connected terms (C1b) with ij as

$$\begin{aligned}m^2_\Gamma(\vec{q}\,) = \frac{LN_G}{N_{\vec{q}}}\sum_{\mathfrak{D}_1,\mathfrak{D}_2,\mathfrak{D}_3}&\left[\vec{M}(\Gamma)\cdot\left(\hat{1}-\tilde{\Omega}(\vec{0}\,)\cdot\tilde{x}\right)\right]_{\mathfrak{D}_1}\left(W^{\mathfrak{D}_1}_{\mathfrak{D}_2,\mathfrak{D}_3}(\vec{q}\,) + W^{\mathfrak{D}_1}_{\mathfrak{D}_3,\mathfrak{D}_2}(\vec{q}\,)\right)\\ &\times\left[\left(\hat{1}+\tilde{x}\cdot\tilde{\Omega}(\vec{q}\,)\right)\cdot\vec{S}^+\right]_{\mathfrak{D}_2}\left[\left(\hat{1}+\tilde{x}\cdot\tilde{\Omega}(\vec{q}\,)\right)\cdot\vec{S}^-\right]_{\mathfrak{D}_3}\end{aligned} \tag{C10a}$$

$$m^3_\Gamma(\vec{q}\,) = \frac{LN_G}{N_{\vec{q}}}\sum_{\mathfrak{D}_1,\mathfrak{D}_2,\mathfrak{D}_3}\left[\vec{M}(\Gamma)\cdot\tilde{\Omega}(\vec{0}\,)\right]_{\mathfrak{D}_1}\tilde{\xi}^{\mathfrak{D}_2,\mathfrak{D}_3}_{\mathfrak{D}_1}\left[\tilde{\Omega}(\vec{q}\,)\cdot\vec{S}^+\right]_{\mathfrak{D}_2}\left[\tilde{\Omega}(\vec{q}\,)\cdot\vec{S}^-\right]_{\mathfrak{D}_3} \tag{C10b}$$

$$m^4_\Gamma(\vec{q}\,) = \frac{LN_G}{N_{\vec{q}}}\vec{M}(\Gamma)\cdot\tilde{\Omega}(\vec{0}\,)\cdot(\overset{+}{T}\cdot\tilde{\Omega}(\vec{q}\,)\cdot\vec{S}^- + \overset{-}{T}\cdot\tilde{\Omega}(\vec{q}\,)\cdot\vec{S}^+) \tag{C10c}$$

$$m^5_\Gamma(\vec{q}\,) = \frac{LN_G}{N_{\vec{q}}}\vec{S}^+ \cdot \tilde{\Omega}(\vec{q}\,) \cdot \tilde{M}(\Gamma) \cdot \tilde{\Omega}(\vec{q}\,) \cdot \vec{S}^- \tag{C10d}$$

The tensors $W^{\mathfrak{D}_1}_{\mathfrak{D}_2,\mathfrak{D}_3}(\vec{q}\,)$, $\tilde{\xi}^{\mathfrak{D}_2,\mathfrak{D}_3}_{\mathfrak{D}_1}$ are defined in appendix B. In figure 4 all diagrams, which belong to the atomic interactions are presented.

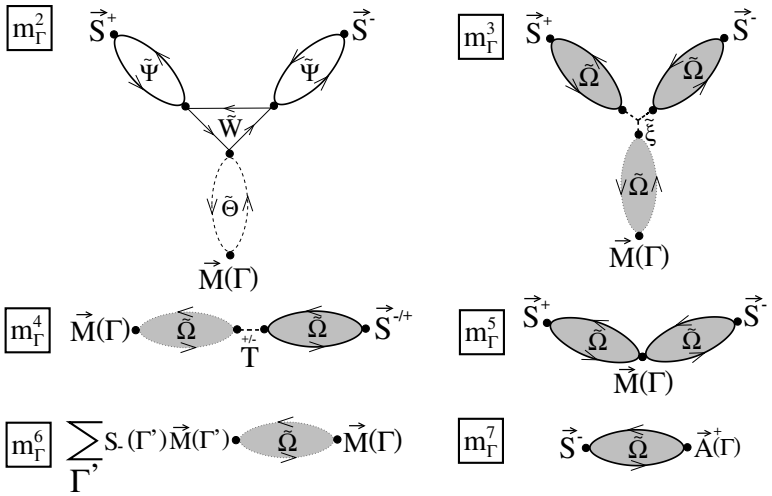

Figure 4. All contributing diagrams in the evaluation of the atomic energy. The diagrams $\tilde{\Phi}(\vec{q})$ and $\tilde{\Psi}(\vec{q})$ are defined as $\tilde{\Phi} = \hat{1} - \tilde{\Omega} \cdot \tilde{x}$, $\tilde{\Psi} = \hat{1} + \tilde{x} \cdot \tilde{\Omega}$. Dotted and solid lines indicate the arguments $\vec{0}$ and $\vec{q}$, respectively.

The connected diagrams in (C1*b*) with $i = j$ are determined by the external vertex-operator

$$\hat{P}_G \hat{S}^+ \hat{S}^- \hat{P}_G = \sum_{\Gamma'} \lambda^2_{\Gamma'} S_-(\Gamma') \hat{m}_{\Gamma'}. \tag{C11}$$

This expression leads to the contribution

$$m^6_\Gamma(\vec{q}\,) = \frac{LN_G}{N_{\vec{q}}} \sum_{\Gamma'} S_-(\Gamma') \left[\vec{M}(\Gamma') \cdot \tilde{\Omega}(\vec{0}\,) \cdot \vec{M}(\Gamma) \right] = m^6_\Gamma(\vec{0}\,). \tag{C12}$$

For the evaluation of (C1*c*), we need the external vertex for the operator $\hat{P}_G \hat{S}^+ \hat{m}_\Gamma \hat{P}_G$, which is the same as the respective term in (52*a*) for fixed Γ,

$$A^+_{(\sigma_1\sigma_2)} \equiv \lambda_{\Gamma_+} \lambda_\Gamma \sqrt{S_+(\Gamma)} \sum_{I_1,I_2} T_{I_1,\Gamma_+} T^+_{\Gamma,I_2} \mathfrak{V}^{(\sigma_1\sigma_2)}_{I_1,I_2}. \tag{C13}$$

The only connected diagram in (C1*c*) is therefore given as

$$m^7_\Gamma(\vec{q}) = \frac{LN_G}{N_{\vec{q}}} \left(\vec{A}^+ \cdot \tilde{\Omega}(\vec{q}) \cdot \vec{S}^- + \text{c.c.} \right). \tag{C14}$$

Finally, we determine the contribution (C1*d*) as

$$m^8_\Gamma(\vec{q}) = \frac{LN_G}{N_{\vec{q}}} S_+(\Gamma) m_{\Gamma_+} = m^8_\Gamma(\vec{0}). \tag{C15}$$

Here, we used the relation

$$\hat{S}^+ \hat{m}_\Gamma \hat{S}^- = S_+(\Gamma) \hat{m}_{\Gamma_+}. \tag{C16}$$

To summarize, the expectation value (C1d) for the atomic energy is given as

$$\frac{\left\langle \Psi_{\vec{q}}^{\mathrm{G}} \left| \hat{H}_{\mathrm{at}} \right| \Psi_{\vec{q}}^{\mathrm{G}} \right\rangle}{N_{\vec{q}}} = L \sum_{\Gamma} E_{\Gamma} m_{\Gamma} + \sum_{\Gamma} E_{\Gamma} \sum_{c=1}^{8} m_{\Gamma}^{c}(\vec{q}). \tag{C17}$$

Appendix D. Evaluation of the one-particle energy

For the diagrammatic evaluation of the one-particle-energy we write the expectation value (28b) as

$$\frac{\left\langle \Psi_{\vec{q}}^{G} \left| \hat{H}_{1} \right| \Psi_{\vec{q}}^{G} \right\rangle}{N_{\vec{q}}} = \frac{1}{N_{\vec{q}}} \sum_{k(\neq)l} \sum_{\sigma_k,\sigma_l} t_{k,l}^{\sigma_k,\sigma_l} \Bigg\{ \sum_{i,\, j(\neq k,l)} \mathrm{e}^{\mathrm{i}\vec{q}(\vec{R}_i - \vec{R}_j)} \left\langle \hat{S}_i^{+} \hat{c}_{k;\sigma_k}^{+} \hat{c}_{l;\sigma_l} \hat{S}_j^{-} \right\rangle_{\Psi_{\mathrm{G}}} \tag{D1a}$$

$$+ \sum_{i(\neq k,l)} \left(\mathrm{e}^{\mathrm{i}\vec{q}(\vec{R}_i - \vec{R}_l)} \left\langle \hat{S}_i^{+} \hat{c}_{k;\sigma_k}^{+} \hat{c}_{l;\sigma_l} \hat{S}_l^{-} \right\rangle_{\Psi_{\mathrm{G}}} + \mathrm{e}^{\mathrm{i}\vec{q}(\vec{R}_i - \vec{R}_k)} \left\langle \hat{S}_i^{+} \hat{c}_{k;\sigma_k}^{+} \hat{c}_{l;\sigma_l} \hat{S}_k^{-} \right\rangle_{\Psi_{\mathrm{G}}} \right) + \mathrm{c.c.} \tag{D1b}$$

$$+ \left(\mathrm{e}^{\mathrm{i}\vec{q}(\vec{R}_k - \vec{R}_l)} \left\langle \hat{S}_k^{+} \hat{c}_{k;\sigma_k}^{+} \hat{c}_{l;\sigma_l} \hat{S}_l^{-} \right\rangle_{\Psi_{\mathrm{G}}} + \mathrm{e}^{\mathrm{i}\vec{q}(\vec{R}_l - \vec{R}_k)} \left\langle \hat{c}_{k;\sigma_k}^{+} \hat{S}_k^{-} \hat{S}_l^{+} \hat{c}_{l;\sigma_l} \right\rangle_{\Psi_{\mathrm{G}}} \right) + \mathrm{c.c.} \tag{D1c}$$

$$+ \left\langle \hat{S}_k^{+} \hat{c}_{k;\sigma_k}^{+} \hat{S}_k^{-} \hat{c}_{l;\sigma_l} \right\rangle_{\Psi_{\mathrm{G}}} + \mathrm{c.c.} \Bigg\}. \tag{D1d}$$

Here, we already used the fact that the tight-binding parameters do not contain any local terms. In (D1a) we have to distinguish connected and unconnected diagrams. The unconnected contributions may be written as

$$(D1a)^{\mathrm{uc}} = \frac{1}{N_{\vec{q}}} \sum_{k \neq l} \sum_{\sigma_k,\sigma_l} t_{k,l}^{\sigma_k,\sigma_l} \left\langle \hat{c}_{k;\sigma_k}^{+} \hat{c}_{l;\sigma_l} \right\rangle_{\Psi_{\mathrm{G}}} \Bigg[\sum_{i \neq j(\neq k,l)} \mathrm{e}^{\mathrm{i}\vec{q}(\vec{R}_i - \vec{R}_j)} \tag{D2}$$

$$\times \left\langle \left(\hat{P}_{i;\mathrm{G}} \hat{S}_i^{+} \hat{P}_{i;\mathrm{G}} \right) \left(\hat{P}_{j;\mathrm{G}} \hat{S}_j^{-} \hat{P}_{j;\mathrm{G}} \right) \times \prod_{m(\neq i,j,k,l)} \hat{P}_{m;\mathrm{G}}^{2} \right\rangle_{\Phi_0}$$

$$+ \sum_{i} \left\langle \left(\hat{P}_{i;\mathrm{G}} \hat{S}_i^{+} \hat{S}_i^{-} \hat{P}_{i;\mathrm{G}} \right) \prod_{m(\neq i,k,l)} \hat{P}_{m;\mathrm{G}}^{2} \right\rangle_{\Phi_0} \Bigg].$$

Equation (D2) can be evaluated, using the same arguments as discussed in connection with equation (C2). This evaluation leads to

$$(D1a)^{\mathrm{uc}} = E_{\mathrm{kin}} - \varepsilon^{1}(\vec{q}\,) \tag{D3a}$$

$$\varepsilon^{1}(\vec{q}\,) = \frac{2E_{\mathrm{kin}}}{L} \frac{LN_{\mathrm{G}}}{N_{\vec{q}}} \left(2\vec{S}^{+} \cdot \tilde{\Omega}(\vec{q}\,) \cdot \vec{S}^{-} + \sum_{\Gamma'} S_{-}(\Gamma') m_{\Gamma'} + \vec{S}^{+} \cdot \tilde{\Omega}(\vec{q}\,) \cdot \tilde{x} \cdot \tilde{\Omega}(\vec{q}\,) \cdot \vec{S}^{-} \right) \tag{D3b}$$

where

$$E_{\mathrm{kin}} = \sum_{k \neq l} \sum_{\sigma_k,\sigma_l} t_{k,l}^{\sigma_k,\sigma_l} \left\langle \hat{c}_{k;\sigma_k}^{+} \hat{c}_{l;\sigma_l} \right\rangle_{\Psi_{\mathrm{G}}}. \tag{D4}$$

Before we start to discuss the connected diagrams, we should first consider the general structure of external vertices in (D1a) at lattice sites k and l, where electrons are created or annihilated. For example, the vertex-function of the operator $\hat{c}_{\sigma}^{+}$ leads to

$$\left\{ \ldots \hat{P}_{\mathrm{G}} \hat{c}_{\sigma}^{+} \hat{P}_{\mathrm{G}} \ldots \right\}_{\Phi_0}^{C} = \sum_{\Gamma,\Gamma'} \lambda_{\Gamma} \lambda_{\Gamma'} \sum_{I(\sigma \notin I)} f_{\sigma}^{I} T_{\Gamma,I\cup\sigma}^{+} T_{I,\Gamma'} \sum_{I_1,I_2} T_{I_1,\Gamma} T_{\Gamma',I_2}^{+} \left\{ \ldots \hat{m}_{I_1,I_2} \ldots \right\}_{\Phi}^{C}. \tag{D5}$$

Hence, our general problem is the calculation of vertex-contributions for operators $\hat{m}_{I_1,I_2}$ with $|I_1| - |I_2| = 1$. The first case is a vertex with only one incoming and no outgoing line,

$$\{\ldots \hat{m}_{I_1,I_2} \ldots\}^C_{\Phi_0} \to \sum_{\sigma'} \mathfrak{h}_{I_1,I_2}(\sigma') \{\ldots \hat{c}^+_{\sigma'} \ldots\}^c_{\Phi_0} \tag{D6a}$$

$$\mathfrak{h}_{I_1,I_2}(\sigma') = \frac{1}{1-n^0_{\sigma'}} \sum_{I(\sigma' \notin I)} f^I_{\sigma'} m^0_I \delta^{I\cup\sigma'}_{I_1} \delta^I_{I_2}. \tag{D6b}$$

Note that equation (D5) together with (D6) yields directly the q-factor (16b), which occurs as the renormalization factor for hopping processes.

Furthermore we have the cases with two (three) incoming and one (two) outgoing lines. These processes lead to the vertices

$$\{\ldots \hat{m}_{I_1,I_2} \ldots\}^C_{\Phi_0} \to \sum_{\sigma'} \sum_{\sigma_1,\sigma_2} \mathfrak{H}^{(\sigma_1,\sigma_2)}_{I_1,I_2}(\sigma') \{\ldots (\hat{c}^+_{\sigma'})(\hat{c}^+_{\sigma_1}\hat{c}_{\sigma_2}) \ldots\}^c_{\Phi_0} \tag{D7a}$$

$$\mathfrak{H}^{(\sigma_1\sigma_2)}_{I_1,I_2}(\sigma') = \sum_{I(\sigma',\sigma_1,\sigma_2 \notin I)} f^I_{\sigma'} f^I_{\sigma_1} f^I_{\sigma_2} m^0_I \Big(\prod_{\sigma \in (\sigma',\sigma_1,\sigma_2)} \frac{1}{(1-n^0_\sigma)} \Big) \tag{D7b}$$
$$\times \Big[f^{\sigma_1}_{\sigma'} \delta^{I\cup(\sigma',\sigma_1)}_{I_1,} \delta^{I\cup\sigma_2}_{I_2} - \delta^{\sigma_2}_{\sigma_1} \delta^{I\cup\sigma'}_{I_1} \delta^I_{I_2} + \delta^{\sigma_2}_{\sigma'} \delta^{I\cup\sigma_1}_{I_1} \delta^I_{I_2} \Big].$$

and

$$\{\ldots \hat{m}_{I_1,I_2} \ldots\}^C_{\Phi_0} \to \sum_{\sigma'} \sum_{\sigma_1,\sigma_2,\sigma_3,\sigma_4} \mathfrak{H}^{(\sigma_1\sigma_2)(\sigma_3\sigma_4)}_{I_1,I_2}(\sigma') \{\ldots (\hat{c}^+_{\sigma'})(\hat{c}^+_{\sigma_1}\hat{c}_{\sigma_2})(\hat{c}^+_{\sigma_3}\hat{c}_{\sigma_4}) \ldots\}^c_{\Phi_0} \tag{D8a}$$

$$\mathfrak{H}^{(\sigma_1\sigma_2)(\sigma_3\sigma_4)}_{I_1,I_2}(\sigma')$$
$$= \sum_{I(\sigma_1,\sigma_2,\sigma_3,\sigma_4,\sigma' \notin I)} f^I_{\sigma_1} f^I_{\sigma_2} f^I_{\sigma_3} f^I_{\sigma_4} f^I_{\sigma'} m^0_I \Big(\prod_{\sigma \in (\sigma_1,\sigma_2,\sigma_3,\sigma_4,\sigma')} \frac{1}{(1-n^0_\sigma)} \Big) \tag{D8b}$$
$$\times f^{\sigma_1}_{\sigma'} f^{\sigma_3}_{\sigma'} \Big[f^{\sigma_3}_{\sigma_1} f^{\sigma_4}_{\sigma_2} \delta^{I_1}_{I\cup(\sigma_1,\sigma_3,\sigma')} \delta^{I_2}_{I\cup(\sigma_2,\sigma_4),} - f^{\sigma_1}_{\sigma'} \Big(\delta^{\sigma_2}_{\sigma_1} \delta^{I_1}_{I\cup(\sigma_3,\sigma')} \delta^{I_2}_{I\cup\sigma_4}$$
$$- \delta^{\sigma_4}_{\sigma_1} \delta^{I_1}_{I\cup(\sigma_3,\sigma')} \delta^{I_2}_{I\cup\sigma_2} \Big) + f^{\sigma_3}_{\sigma'} \Big(\delta^{\sigma_3}_{\sigma_2} \delta^{I_1}_{I\cup(\sigma_1,\sigma')} \delta^{I_2}_{I\cup\sigma_4} - \delta^{\sigma_4}_{\sigma_3} \delta^{I_1}_{I\cup(\sigma_1,\sigma')} \delta^{I_2}_{I\cup\sigma_2} \Big)$$
$$+ f^{\sigma_1}_{\sigma'} f^{\sigma_3}_{\sigma'} (\delta^{\sigma_2}_{\sigma_1} \delta^{\sigma_4}_{\sigma_3} - \delta^{\sigma_3}_{\sigma_2} \delta^{\sigma_4}_{\sigma_1}) \delta^{I_1}_{I\cup\sigma'} \delta^{I_2}_I$$
$$+ \delta^{\sigma_2}_{\sigma'} f^{\sigma_1}_{\sigma'} f^{\sigma_3}_{\sigma'} \Big(f^{\sigma_3}_{\sigma_1} \delta^{I_1}_{I\cup(\sigma_1,\sigma_3)} \delta^{I_2}_{I\cup\sigma_4} - \delta^{\sigma_4}_{\sigma_3} \delta^{I_1}_{I\cup\sigma_1} \delta^{I_2}_I + \delta^{\sigma_4}_{\sigma_1} \delta^{I_1}_{I\cup\sigma_3} \delta^{I_2}_I \Big)$$
$$- \delta^{\sigma_4}_{\sigma'} f^{\sigma_1}_{\sigma'} f^{\sigma_3}_{\sigma'} \Big(f^{\sigma_3}_{\sigma_1} \delta^{I_1}_{I\cup(\sigma_1,\sigma_3)} \delta^{I_2}_{I\cup\sigma_2} - \delta^{\sigma_2}_{\sigma_3} \delta^{I_1}_{I\cup\sigma_1} \delta^{I_2}_I + \delta^{\sigma_2}_{\sigma_1} \delta^{I_1}_{I\cup\sigma_3} \delta^{I_2}_I \Big) \Big].$$

Using (D5) we may now define the following vertex-functions for a single creation-operator as it occurs in (D1a)

$$Q^+_{\mathfrak{D}}(\sigma,\sigma') = \sum_{\Gamma,\Gamma'} \lambda_\Gamma \lambda_{\Gamma'} \sum_{I(\sigma \notin I)} f^I_\sigma T^+_{\Gamma,I\cup\sigma} T_{I,\Gamma'} \sum_{I_1,I_2} T_{I_1,\Gamma} T^+_{\Gamma',I_2} \mathfrak{H}^{\mathfrak{D}}_{I_1,I_2}(\sigma'), \tag{D9a}$$

$$\tilde{Q}^+_{\mathfrak{D}\mathfrak{D}'}(\sigma,\sigma') = \sum_{\Gamma,\Gamma'} \lambda_\Gamma \lambda_{\Gamma'} \sum_{I(\sigma \notin I)} f^I_\sigma T^+_{\Gamma,I\cup\sigma} T_{I,\Gamma'} \sum_{I_1,I_2} T_{I_1,\Gamma} T^+_{\Gamma',I_2} \mathfrak{H}^{\mathfrak{D}\mathfrak{D}'}_{I_1,I_2}(\sigma') \tag{D9b}$$

The respective vertices $Q_{\mathfrak{D}}(\sigma,\sigma')$, $\tilde{Q}_{\mathfrak{D}\mathfrak{D}'}(\sigma,\sigma')$ for annihilation-operators are given as

$$Q_{(\sigma_1\sigma_2)}(\sigma,\sigma') = \Big[Q^+_{(\sigma_2\sigma_1)}(\sigma,\sigma') \Big]^* \tag{D10a}$$

$$\tilde{Q}_{(\sigma_1\sigma_2)(\sigma_3\sigma_4)}(\sigma,\sigma') = \Big[\tilde{Q}^+_{(\sigma_2\sigma_1)(\sigma_4\sigma_3)}(\sigma,\sigma') \Big]^*. \tag{D10b}$$

Now we can determine the connected diagrams in (D1a). First, we have the following terms for $i\ j$

$$\varepsilon^2(\vec{q}) = \frac{N_{\rm G}}{N_{\vec{q}}} \sum_{\sigma_1,\sigma_2} \sqrt{q_{\sigma_1} q_{\sigma_2}} \sum_{\mathfrak{D}_1,\mathfrak{D}_2} \left(\tilde{U}^{\sigma_1,\sigma_2}_{\mathfrak{D}_1,\mathfrak{D}_2}(\vec{q}) + \tilde{U}^{\sigma_1,\sigma_2}_{\mathfrak{D}_2,\mathfrak{D}_1}(\vec{q}) \right) \times [(\hat{1} + \tilde{x}\cdot\tilde{\Omega}(\vec{q}))\cdot\vec{S}^+]_{\mathfrak{D}_1}[(\hat{1} + \tilde{x}\cdot\tilde{\Omega}(\vec{q}))\cdot\vec{S}^-]_{\mathfrak{D}_2} \tag{D11a}$$

$$\varepsilon^3(\vec{q}) = \frac{N_{\rm G}}{N_{\vec{q}}} \sum_{\sigma_1,\sigma_2} \sqrt{q_{\sigma_1} q_{\sigma_2}} \sum_{\mathfrak{D}_1,\mathfrak{D}_2,\mathfrak{D}_3,\mathfrak{D}_4} V^{\mathfrak{D}_1}_{(\sigma_1\sigma_2)(\sigma_1\sigma_2)}(\vec{0})[\tilde{x}\cdot(\hat{1} + \tilde{\Omega}(\vec{0})\cdot\tilde{x})]_{\mathfrak{D}_1,\mathfrak{D}_2} \times \left(\tilde{W}^{\mathfrak{D}_2}_{\mathfrak{D}_3,\mathfrak{D}_4}(\vec{q}) + \tilde{W}^{\mathfrak{D}_2}_{\mathfrak{D}_4,\mathfrak{D}_3}(\vec{q}) \right) \times [(\hat{1} + \tilde{x}\cdot\tilde{\Omega}(\vec{q}))\cdot\vec{S}^+]_{\mathfrak{D}_3}[(\hat{1} + \tilde{x}\cdot\tilde{\Omega}(\vec{q}))\cdot\vec{S}^-]_{\mathfrak{D}_4} \tag{D11b}$$

$$\varepsilon^4(\vec{q}) = \frac{N_G}{N_{\vec{q}}} \sum_{\sigma_1,\sigma_2} \sqrt{q_{\sigma_1} q_{\sigma_2}} \sum_{\mathfrak{D}_1,\mathfrak{D}_2,\mathfrak{D}_3,\mathfrak{D}_4} V^{\mathfrak{D}_1}_{(\sigma_1\sigma_2)(\sigma_1\sigma_2)}(\vec{0})[\hat{1} + \tilde{x}\cdot\tilde{\Omega}(\vec{0})]_{\mathfrak{D}_1,\mathfrak{D}_2} \times \tilde{\xi}^{\mathfrak{D}_3,\mathfrak{D}_4}_{\mathfrak{D}_2}[\tilde{\Omega}(\vec{q})\cdot\vec{S}^+]_{\mathfrak{D}_3}[\tilde{\Omega}(\vec{q})\cdot\vec{S}^-]_{\mathfrak{D}_4} \tag{D11c}$$

$$\varepsilon^5(\vec{q}) = \frac{N_G}{N_{\vec{q}}} \sum_{\sigma_1,\sigma_2,\sigma_1',\sigma_2'} \sum_{\mathfrak{D}_1,\mathfrak{D}_2} \left(Q^+_{\mathfrak{D}_1}(\sigma_1,\sigma_1') Q_{\mathfrak{D}_2}(\sigma_2,\sigma_2') + Q^+_{\mathfrak{D}_2}(\sigma_1,\sigma_1') Q_{\mathfrak{D}_1}(\sigma_2,\sigma_2') \right) \times E^{\sigma_1,\sigma_2}_{\sigma_1',\sigma_2'}(\vec{q})[\tilde{\Omega}(\vec{q})\cdot\vec{S}^+]_{\mathfrak{D}_1}[\tilde{\Omega}(\vec{q})\cdot\vec{S}^-]_{\mathfrak{D}_2} \tag{D11d}$$

$$\varepsilon^6(\vec{q}) = \frac{N_G}{N_{\vec{q}}} \sum_{\sigma_1,\sigma_2,\sigma_1'} \sqrt{q_{\sigma_2}} \sum_{\mathfrak{D}_1,\mathfrak{D}_2} \Big(Q^+_{\mathfrak{D}_1}(\sigma_1,\sigma_1') \bar{V}^{\mathfrak{D}_2}_{(\sigma_1'\sigma_2)(\sigma_1\sigma_2)}(\vec{q}) + Q_{\mathfrak{D}_1}(\sigma_1,\sigma_1') V^{\mathfrak{D}_2}_{(\sigma_2\sigma_1')(\sigma_2\sigma_1)}(\vec{q}) \Big) \times \Big\{ \Big[\left(\hat{1} + \tilde{x}\cdot\tilde{\Omega}(\vec{q})\right)\cdot\vec{S}^+ \Big]_{\mathfrak{D}_2} \Big[\tilde{\Omega}(\vec{q})\cdot\vec{S}^- \Big]_{\mathfrak{D}_1} + \Big[\tilde{\Omega}(\vec{q})\cdot\vec{S}^+ \Big]_{\mathfrak{D}_1} \Big[\left(\hat{1} + \tilde{x}\cdot\tilde{\Omega}(\vec{q})\right)\cdot\vec{S}^- \Big]_{\mathfrak{D}_2} \Big\} \tag{D11e}$$

$$\varepsilon^7(\vec{q}) = \frac{N_G}{N_{\vec{q}}} \sum_{\sigma_1,\sigma_2,\sigma_1'} \sqrt{q_{\sigma_2}} \sum_{\mathfrak{D}_1,\mathfrak{D}_2,\mathfrak{D}_3,\mathfrak{D}_4} \left(Q^+_{\mathfrak{D}_1}(\sigma_1,\sigma_1') E^{(\sigma_1\sigma_2)}_{(\sigma_1'\sigma_2)}(\vec{0}) + Q_{\mathfrak{D}_1}(\sigma_1,\sigma_1') E^{(\sigma_2\sigma_1)}_{(\sigma_2\sigma_1')}(\vec{0}) \right) \times \Big[\hat{1} + \tilde{\Omega}(\vec{0})\cdot\tilde{x} \Big]_{\mathfrak{D}_1,\mathfrak{D}_2} \left(W^{\mathfrak{D}_2}_{\mathfrak{D}_3,\mathfrak{D}_4}(\vec{q}) + W^{\mathfrak{D}_2}_{\mathfrak{D}_4,\mathfrak{D}_3}(\vec{q}) \right) \times \Big[\left(\hat{1} + \tilde{x}\cdot\tilde{\Omega}(\vec{q})\right)\cdot\vec{S}^+ \Big]_{\mathfrak{D}_3} \Big[\left(\hat{1} + \tilde{x}\cdot\tilde{\Omega}(\vec{q})\right)\cdot\vec{S}^- \Big]_{\mathfrak{D}_4} \tag{D11f}$$

$$\varepsilon^8(\vec{q}) = \frac{N_G}{N_{\vec{q}}} \sum_{\sigma_1,\sigma_2,\sigma_1'} \sqrt{q_{\sigma_2}} \sum_{\mathfrak{D}_1,\mathfrak{D}_2,\mathfrak{D}_3,\mathfrak{D}_4} \left(Q^+_{\mathfrak{D}_1}(\sigma_1,\sigma_1') E^{(\sigma_1\sigma_2)}_{(\sigma_1'\sigma_2)}(\vec{0}) + Q_{\mathfrak{D}_1}(\sigma_1,\sigma_1') E^{(\sigma_2\sigma_1)}_{(\sigma_2\sigma_1')}(\vec{0}) \right) \times \tilde{\Omega}^{\mathfrak{D}_2}_{\mathfrak{D}_1}(\vec{0})\tilde{\xi}^{\mathfrak{D}_3,\mathfrak{D}_4}_{\mathfrak{D}_2}[\tilde{\Omega}(\vec{q})\cdot\vec{S}^+]_{\mathfrak{D}_3}[\tilde{\Omega}(\vec{q})\cdot\vec{S}^-]_{\mathfrak{D}_4} \tag{D11g}$$

$$\varepsilon^9(\vec{q}) = \frac{N_G}{N_{\vec{q}}} \sum_{\sigma_1,\sigma_2,\sigma_1'} \sqrt{q_{\sigma_2}} \sum_{\mathfrak{D}_1,\mathfrak{D}_2} \left(\tilde{Q}^+_{\mathfrak{D}_1\mathfrak{D}_2}(\sigma_1,\sigma_1') E^{(\sigma_1\sigma_2)}_{(\sigma_1'\sigma_2)}(\vec{0}) + \tilde{Q}_{\mathfrak{D}_1\mathfrak{D}_2}(\sigma_1,\sigma_1') E^{(\sigma_2\sigma_1)}_{(\sigma_2\sigma_1')}(\vec{0}) \right) \times [\tilde{\Omega}(\vec{q})\cdot\vec{S}^+]_{\mathfrak{D}_1}[\tilde{\Omega}(\vec{q})\cdot\vec{S}^-]_{\mathfrak{D}_2} \tag{D11h}$$

$$\varepsilon^{10}(\vec{q}) = \frac{N_G}{N_{\vec{q}}} \sum_{\sigma_1,\sigma_2,\sigma_1'} \sqrt{q_{\sigma_2}} \sum_{\mathfrak{D}_1} \left(Q^+_{\mathfrak{D}_1}(\sigma_1,\sigma_1') E^{(\sigma_1\sigma_2)}_{(\sigma_1'\sigma_2)}(\vec{0}) + Q_{\mathfrak{D}_1}(\sigma_1,\sigma_1') E^{(\sigma_2\sigma_1)}_{(\sigma_2\sigma_1')}(\vec{0}) \right) \times [\tilde{\Omega}(\vec{q})\cdot(\overset{+}{T}\cdot\tilde{\Omega}(\vec{q})\cdot\vec{S}^- + \overset{-}{T}\cdot\tilde{\Omega}(\vec{q})\cdot\vec{S}^+)]_{\mathfrak{D}_1} \tag{D11i}$$

$$\varepsilon^{11}(\vec{q}\,) = \frac{N_G}{N_{\vec{q}}} \sum_{\sigma_1,\sigma_2} \sqrt{q_{\sigma_1} q_{\sigma_2}} \sum_{\mathfrak{D}_1} V^{\mathfrak{D}_1}_{(\sigma_1\sigma_2)(\sigma_1\sigma_2)}(\vec{0}\,)$$
$$\times[(\hat{1} + \tilde{x}\cdot\tilde{\Omega}(\vec{q}\,))\cdot(\overset{+}{T}\cdot\tilde{\Omega}(\vec{q}\,)\cdot\vec{S}^{-} + \overset{-}{T}\cdot\tilde{\Omega}(\vec{q}\,)\cdot\vec{S}^{+})]_{\mathfrak{D}_1}. \tag{D11j}$$

Expressions for the diagrams $E^{\mathfrak{D}_1}_{\mathfrak{D}_2}$, $U^{\mathfrak{D}_1}_{\mathfrak{D}_2\mathfrak{D}_3}$, $V^{\mathfrak{D}_1}_{\mathfrak{D}_2\mathfrak{D}_3}$, and $\bar{V}^{\mathfrak{D}_1}_{\mathfrak{D}_2\mathfrak{D}_3}$ can be found in appendix B. Using equation (C11) we derive the connected diagrams in (D1a) with $i = j$ as

$$\varepsilon^{12}(\vec{q}\,) = \frac{N_{\mathrm{G}}}{N_{\vec{q}}} \sum_{\sigma_1,\sigma_2} \sqrt{q_{\sigma_1} q_{\sigma_2}} \sum_{\mathfrak{D}_1} \sum_{\Gamma'} \lambda^2_{\Gamma'} S_-(\Gamma') V^{\mathfrak{D}_1}_{(\sigma_1\sigma_2)(\sigma_1\sigma_2)}(\vec{0}\,) \left[\left(\hat{1} + \tilde{x}\cdot\tilde{\Omega}(\vec{0}\,)\right)\cdot\vec{M}(\Gamma')\right] \tag{D12a}$$

$$\varepsilon^{13}(\vec{q}\,) = \frac{N_{\mathrm{G}}}{N_{\vec{q}}} \sum_{\sigma_1,\sigma_2,\sigma_1'} \sqrt{q_{\sigma_2}} \sum_{\mathfrak{D}_1} \sum_{\Gamma'} \lambda^2_{\Gamma'} S_-(\Gamma') \Big(Q^{+}_{\mathfrak{D}_1}(\sigma_1,\sigma_1') E^{(\sigma_1\sigma_2)}_{(\sigma_1'\sigma_2)}(\vec{0}\,)$$
$$+ Q_{\mathfrak{D}_1}(\sigma_1,\sigma_1') E^{(\sigma_2\sigma_1)}_{(\sigma_2\sigma_1')}(\vec{0}\,)\Big) \left[\tilde{\Omega}(\vec{0}\,)\cdot\vec{M}(\Gamma')\right]_{\mathfrak{D}_1}. \tag{D12b}$$

For the evaluation of (D1b) we need the vertex-function for the operators

$$\hat{P}_{\mathrm{G}}\hat{c}_\sigma\hat{S}^{-}\hat{P}_{\mathrm{G}} = \sum_{\Gamma,\Gamma'} \lambda_\Gamma\lambda_{\Gamma'}\sqrt{S_-(\Gamma')} \sum_{I(\sigma\notin I)} f^I_\sigma T^{+}_{\Gamma,I} T_{I\cup\sigma,\Gamma'_-} \sum_{I_1,I_2} T_{I_1,\Gamma} T^{+}_{\Gamma',I_2} \hat{m}_{I_1,I_2} \tag{D13a}$$

$$\hat{P}_{\mathrm{G}}\hat{c}^{+}_\sigma\hat{S}^{-}\hat{P}_{\mathrm{G}} = \sum_{\Gamma,\Gamma'} \lambda_\Gamma\lambda_{\Gamma'}\sqrt{S_-(\Gamma')} \sum_{I(\sigma\notin I)} f^I_\sigma T^{+}_{\Gamma,I\cup\sigma} T_{I,\Gamma'_-} \sum_{I_1,I_2} T_{I_1,\Gamma} T^{+}_{\Gamma',I_2} \hat{m}_{I_1,I_2} \tag{D13b}$$

with one (or two) incoming or outgoing lines. These functions follow directly from equations (D7a) and (D8a)

$$r(\sigma,\sigma') = \sum_{\Gamma,\Gamma'} \lambda_\Gamma\lambda_{\Gamma'}\sqrt{S_-(\Gamma')} \sum_{I(\sigma\notin I)} f^I_\sigma T^{+}_{\Gamma,I} T_{I\cup\sigma,\Gamma'_-} \sum_{I_1,I_2} T_{I_1,\Gamma} T^{+}_{\Gamma',I_2} \mathfrak{h}_{I_2,I_1}(\sigma') \tag{D14a}$$

$$r^{+}(\sigma,\sigma') = \sum_{\Gamma,\Gamma'} \lambda_\Gamma\lambda_{\Gamma'}\sqrt{S_-(\Gamma')} \sum_{I(\sigma\notin I)} f^I_\sigma T^{+}_{\Gamma,I\cup\sigma} T_{I,\Gamma'_-} \sum_{I_1,I_2} T_{I_1,\Gamma} T^{+}_{\Gamma',I_2} \mathfrak{h}_{I_1,I_2}(\sigma') \tag{D14b}$$

$$R_{\sigma_1,\sigma_2}(\sigma,\sigma') = \sum_{\Gamma,\Gamma'} \lambda_\Gamma\lambda_{\Gamma'}\sqrt{S_-(\Gamma')} \sum_{I(\sigma\notin I)} f^I_\sigma T^{+}_{\Gamma,I} T_{I\cup\sigma,\Gamma'_-} \sum_{I_1,I_2} T_{I_1,\Gamma} T^{+}_{\Gamma',I_2} \mathfrak{H}^{(\sigma_2\sigma_1)}_{I_2,I_1}(\sigma') \tag{D14c}$$

$$R^{+}_{(\sigma_1\sigma_2)}(\sigma,\sigma') = \sum_{\Gamma,\Gamma'} \lambda_\Gamma\lambda_{\Gamma'}\sqrt{S_-(\Gamma')} \sum_{I(\sigma\notin I)} f^I_\sigma T^{+}_{\Gamma,I\cup\sigma} T_{I,\Gamma'_-} \sum_{I_1,I_2} T_{I_1,\Gamma} T^{+}_{\Gamma',I_2} \mathfrak{H}^{(\sigma_1\sigma_2)}_{I_1,I_2}(\sigma'). \tag{D14d}$$

Note that for the vertices of the remaining operators $\hat{P}_{\mathrm{G}}\hat{S}^{+}\hat{c}_\sigma\hat{P}_{\mathrm{G}}$ and $\hat{P}_{\mathrm{G}}\hat{S}^{+}\hat{c}^{+}_\sigma\hat{P}_{\mathrm{G}}$ the rules (D10) apply. Now we are able to summarize the contributions (D1b) as

$$\varepsilon^{14}(\vec{q}\,) = \frac{N_{\mathrm{G}}}{N_{\vec{q}}} \sum_{\sigma_1,\sigma_2,\sigma_1'} \sqrt{q_{\sigma_2}} \sum_{\mathfrak{D}_1} \left(r^{+}(\sigma_1,\sigma_1') \bar{V}^{\mathfrak{D}_1}_{(\sigma_1'\sigma_2)(\sigma_1\sigma_2)}(\vec{q}\,) + r(\sigma_1,\sigma_1') V^{\mathfrak{D}_1}_{(\sigma_2\sigma_1')(\sigma_2\sigma_1)}(\vec{q}\,)\right)$$
$$\times[(\hat{1} + \tilde{x}\cdot\tilde{\Omega}(\vec{q}\,))\cdot\vec{S}^{+}]_{\mathfrak{D}_1} + \mathrm{c.c.} \tag{D15a}$$

$$\varepsilon^{15}(\vec{q}\,) = \frac{N_{\mathrm{G}}}{N_{\vec{q}}} \sum_{\sigma_1,\sigma_2,\sigma_1'} \sqrt{q_{\sigma_2}} \sum_{\mathfrak{D}_1} \left(R^{+}_{\mathfrak{D}_1}(\sigma_1,\sigma_1') E^{(\sigma_1\sigma_2)}_{(\sigma_1'\sigma_2)}(\vec{0}\,) + R_{\mathfrak{D}_1}(\sigma_1,\sigma_1') E^{(\sigma_2\sigma_1)}_{(\sigma_2\sigma_1')}(\vec{0}\,)\right)$$
$$\times[\tilde{\Omega}(\vec{q}\,)\cdot\vec{S}^{+}]_{\mathfrak{D}_1} + \mathrm{c.c.} \tag{D15b}$$

$$\varepsilon^{16}(\vec{q}\,) = \frac{N_{\mathrm{G}}}{N_{\vec{q}}} \sum_{\sigma_1,\sigma_2,\sigma_1',\sigma_2'} \sum_{\mathfrak{D}_1} \left(r^{+}(\sigma_1,\sigma_1') Q_{\mathfrak{D}_1}(\sigma_2,\sigma_2') + r(\sigma_2,\sigma_2') Q^{+}_{\mathfrak{D}_1}(\sigma_1,\sigma_1')\right) E^{(\sigma_1\sigma_2)}_{(\sigma_1'\sigma_2')}(\vec{q}\,)$$
$$\times[\tilde{\Omega}(\vec{q}\,)\cdot\vec{S}^{+}]_{\mathfrak{D}_1} + \mathrm{c.c.}. \tag{D15c}$$

The contributions from equation (D1c) are

$$\varepsilon^{17}(\vec{q}\,) = \frac{N_{\rm G}}{N_{\vec{q}}} \sum_{\sigma_1,\sigma_2,\sigma_1',\sigma_2'} \left(r^{+}(\sigma_1,\sigma_1')\left(r^{+}(\sigma_2,\sigma_2')\right)^{*} + \left(r(\sigma_1,\sigma_1')\right)^{*} r(\sigma_2,\sigma_2')\right) E^{(\sigma_1\sigma_2)}_{(\sigma_1'\sigma_2')}(\vec{q}). \tag{D16}$$

Finally, we need the vertex-function for the operator $\hat{P}_{\rm G}\hat{S}^{+}\hat{c}^{+}_{\sigma}\hat{S}^{-}\hat{P}_{\rm G}$ in (D1d) with one outgoing line

$$l(\sigma,\sigma') = \sum_{\Gamma,\Gamma'} \lambda_{\Gamma}\lambda_{\Gamma'}\sqrt{S_{-}(\Gamma')S_{-}(\Gamma)} \sum_{I(\sigma\notin I)} f^{I}_{\sigma} T^{+}_{\Gamma_{-},I\cup\sigma} T_{I,\Gamma'_{-}} \sum_{I_1,I_2} T_{I_1,\Gamma} T^{+}_{\Gamma',I_2}\mathfrak{h}_{I_1,I_2}(\sigma'). \tag{D17}$$

in (D1d). This gives us the contribution from equation (D1d),

$$\varepsilon^{18}(\vec{q}\,) = \sum_{\sigma_1,\sigma_2,\sigma_1'} \sqrt{q_{\sigma_2}}\, l(\sigma_1,\sigma_1') E^{(\sigma_1\sigma_2)}_{(\sigma_1'\sigma_2)}(\vec{0}) + \text{c.c.} \tag{D18}$$

Altogether we may write the expectation value for the kinetic energy (D1) as

$$\frac{\left\langle \Psi^{\rm G}_{\vec{q}}\, big \middle| \hat{H}_1 \middle| \Psi^{\rm G}_{\vec{q}} \right\rangle}{N_{\vec{q}}} = E_{\rm kin} + \sum_{c=1}^{18} \varepsilon^{c}(\vec{q}). \tag{D19}$$

References

[1] Herring C 1966 *Magnetism* vol IV, ed G T Rado and H Suhl (New York: Academic) p 1
[2] Fazekas P 1999 *Lecture Notes* on Electron Correlation and Magnetism (Singapore: World Scientific)
[3] Stoner E C 1938 *Proc. R. Soc.* A **165** 372
[4] Moruzzi V R, Janak J F and Williams A R 1978 *Calculated Properties of Metals* (New York: Pergamon)
[5] Gutzwiller M C 1963 *Phys. Rev. Lett.* **10** 159
Gutzwiller M C 1964 *Phys. Rev.* **134** A923
Gutzwiller M C 1965 *Phys. Rev.* **137** A1726
[6] Bünemann J, Weber W and Gebhard F 1998 *Phys. Rev.* B **57** 6896
[7] Weber W, Gebhard F and Bünemann J in preparation
[8] Bünemann J, Gebhard F and Weber W 2000 *Found. Phys.* **30** 2011
[9] Mook H A and Nicklow R M 1973 *Phys. Rev.* B **7** 336
[10] Lowde R D and Windsor C G 1970 *Adv. Phys.* **19** 813
[11] Morija T 1985 *Spin Fluctuations in Itinerant Electron Magnetism* (Berlin: Springer)
[12] Cook J F, Lynn J W and Davis H L 1980 *Phys. Rev.* B **21** 4118
[13] Halilov S V, Eschrig H, Perlov A Y andOppeneer P M 1998 *Phys. Rev.* B **58** 293
[14] Morkowski J A 1988 *J. Physique Coll.* **49** 51
[15] Hirsch J E 1997 *Phys. Rev.* B **56** 11022
[16] Wahle J, Blühmer N, Schlipf J, Held K and Vollhardt D 1998 *Phys. Rev.* B **58** 12749
[17] Sugano S, Tanabe Y and Kamimura H 1970 *Multiplets of Transition-Metal Ions in Crystals* (Pure and Applied Physics vol 33) (New York: Academic)
[18] Marshall W and Lovesey S W 1971 *Theory of Thermal Neutron Scattering* (Oxford: Oxford University Press)
[19] Gebhard F 1997 *The Mott Metal–Insulator Transition – Models and Methods* (Springer Tracts in Modern Physics Vol 137) (Berlin: Springer)
[20] Georges A, Kotliar G, Krauth W and Rozenberg M J 1996 *Rev. Mod. Phys.* **68** 13
[21] Bünemann J, Gebhard F and Weber W 1997 *J. Phys.: Condens. Matter* **8** 7343
[22] Slater J C and Koster G F 1954 *Phys. Rev.* **94** 1498
[23] Chen K, Ferrenberg A M and Landau D P 1993 *Phys. Rev.* B **48** 3249
[24] Bloch F 1930 *Z. Phys.* **61** 206